Geochemistry of grey gneiss, tonalite complexes and granitic rocks

The grey gneiss and granitoid rocks were originally separated into a number of mappable units based on their field relationships, mineralogical composition, colour and texture. These field divisions are largely supported by geochemical work presented here, although compositional overlaps were found especially between the dioritic and tonalitic-trondhjemitic groups. In addition, the analytical work revealed the presence of a distinct group of dioritic gneiss not recognised in the field, namely the Qeqertaussaq diorite which occurs

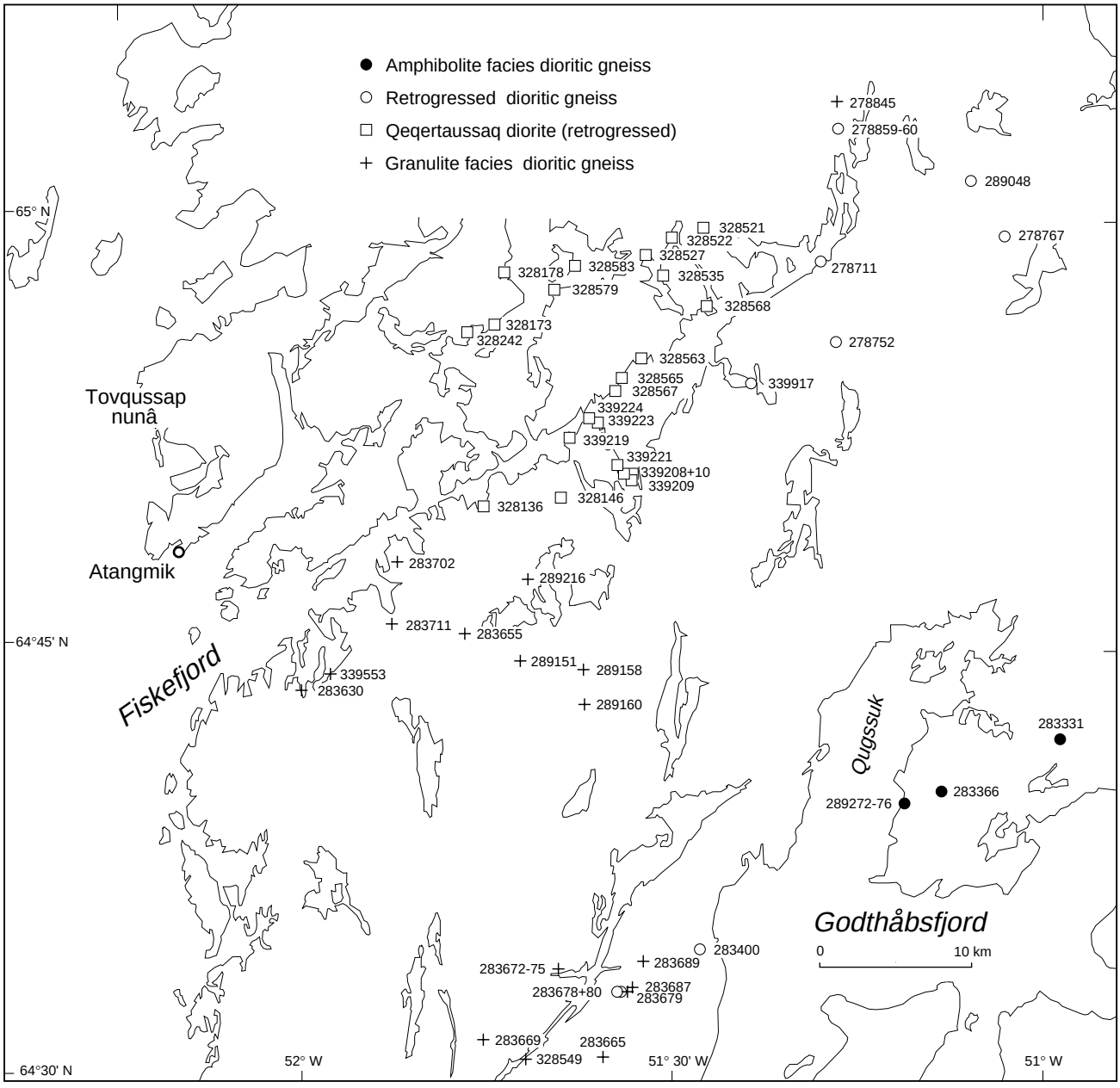

Fig. 52. Locations of analysed dioritic gneiss samples in the Fiskefjord area.

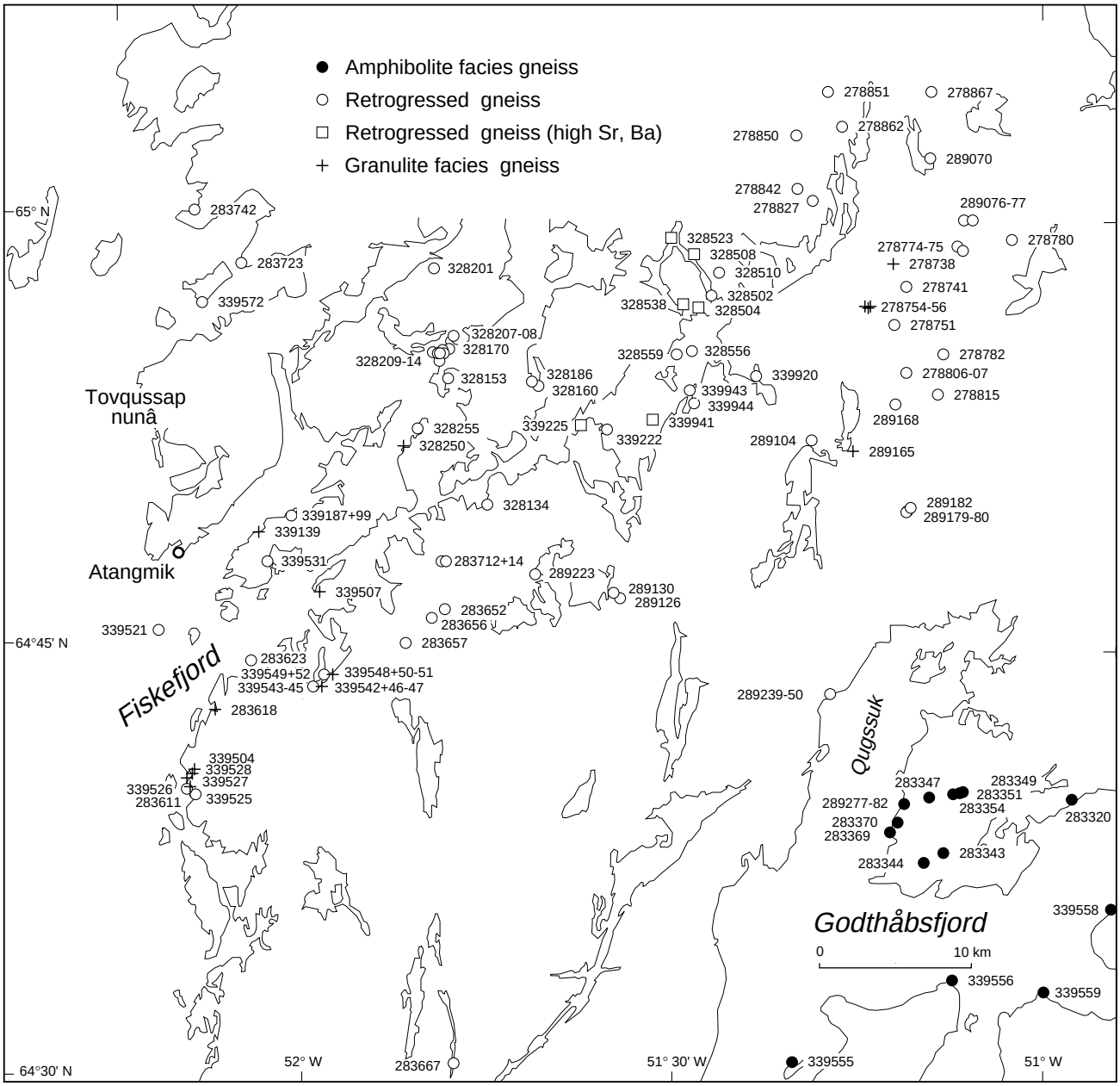

Fig. 53. Locations of analysed samples of tonalitic-trondhjemitic grey gneiss in the Fiskefjord area.

within an area of *c.* 300 km^2 around central Fiskefjord (Fig. 52).

Figures 52 and 53 show sample locations of the main groups of grey gneiss, and Fig. 54, a series of quartz–K-feldspar–plagioclase ternary diagrams (Streckeisen, 1976), gives a first overview of the range of compositions. In Fig. 54 the bulk of the grey gneiss and most samples from the Finnefjeld and Taserssuaq complexes plot in the tonalite-trondhjemite and granodiorite fields; the grey gneiss also comprises rocks in the quartz-dioritic and dioritic fields. The Igánánguit granodiorite and Qugssuk granite largely plot in the granodioritic and granitic fields, respectively.

Figure 54 is based on chemical analyses using the cation norm calculation, with the modification that biotite is introduced when hypersthene and K-feldspar appear together in the norm (6hy + 5or = 8bi + 3qz). Except for the presence of amphibole in some rocks the modified cation norm provides fair estimates of the modes, since orthopyroxene and K-feldspar only rarely occur together. This formal approach to classification gives a reasonable impression of present modal com-

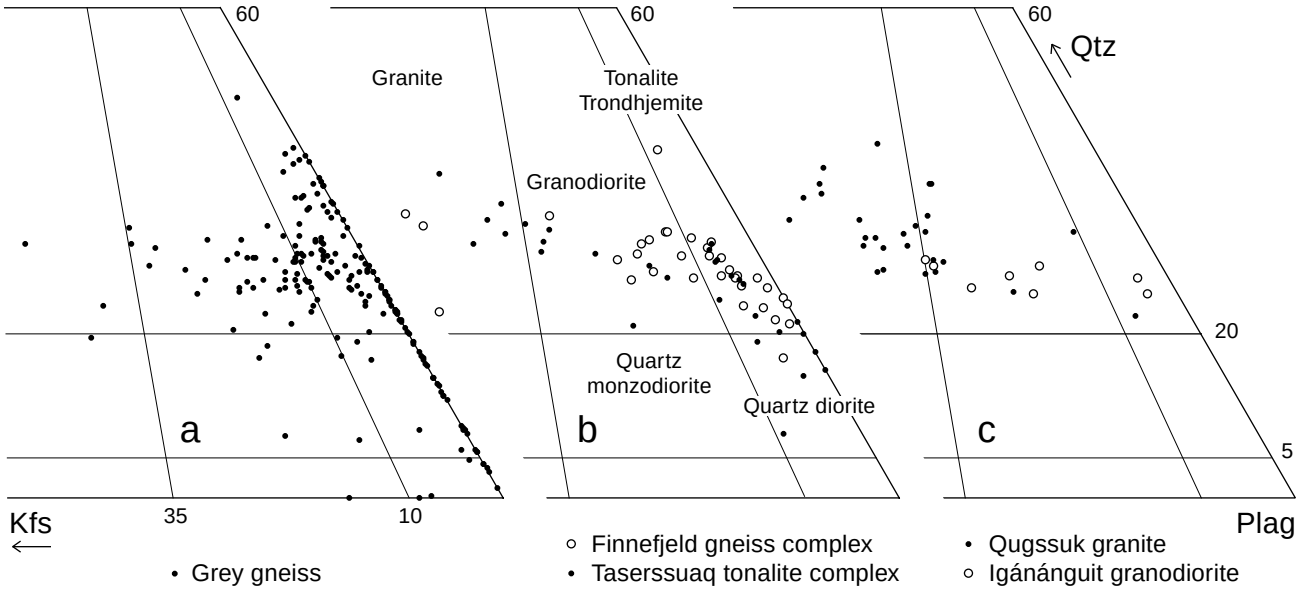

Fig. 54. Quartz–K-feldspar–plagioclase ternary diagrams (Streckeisen, 1976) for Archaean quartzo-feldspathic intrusive rocks in the Fiskefjord area, based on modified cation norm calculations from chemical analyses (see the main text for explanation). (**a**) Grey gneiss, (**b**) Finnefjeld gneiss and Taserssuaq tonalite complexes, (**c**) Igánánguit granodiorite and Qugssuk granite.

positions, but due to element mobility during metamorphic processes it does not reflect the original igneous mineral compositions of all rocks in question.

Common dioritic gneiss and Qeqertaussaq diorite

The grey gneiss covers a large range of compositions from dioritic rocks with less than 55 wt.% SiO_2 to trondhjemitic rocks with over 75% SiO_2; the presentation of geochemical data follows these two large field groups: dioritic gneiss (with less than *c.* 65% SiO_2) and tonalitic-trondhjemitic gneiss (with more than *c.* 63% SiO_2).

Fifty-eight rock samples described in the field as dioritic gneiss (sample locations in Fig. 52) range from *c.* 51 to 65% SiO_2 (Appendixes 5, 6; Fig. 55). They consist of diorite, quartz diorite and mafic tonalite, as well as a few mafic diorites which compositionally resemble andesitic leuco-amphibolites of the supracrustal rock association. The dioritic gneiss comprises two groups with distinctly different geochemical signatures (Figs 55–58): a large group of common dioritic gneiss with general geochemical characteristics similar to those of the tonalitic-trondhjemitic gneiss (which besides the *c.* 3220 Ma Nordlandet dioritic gneiss may also comprise *c.* 3000 Ma old rocks), and the Qeqertaussaq diorite characterised by very high P_2O_5, LREE, Sr and Ba contents (see below).

The common dioritic gneiss, which comprises both amphibolite facies, granulite facies and retrogressed samples, occurs over most of the Fiskefjord area (Fig. 52). Its major and trace element variations against SiO_2 are continuous with those displayed by tonalitic-trondhjemitic grey gneiss (described in detail below), if the latter are extrapolated to lower SiO_2 values (compare Figs 55 and 56 with Figs 59 and 60). Besides, amphibolite facies, granulite facies and retrogressed samples of common dioritic gneiss show some characteristic mutual differences (also found in the tonalitic-trondhjemitic gneiss, see p. 55), namely, low concentrations of LIL elements in granulite facies rocks, large variations of these elements in retrogressed rocks, and high Ba and Sr contents in some retrogressed rocks. However, the relatively small number of samples, the somewhat erratic distribution of SiO_2 contents among them, and the limited number of sample localities make it difficult to establish if there are systematic differences in major element compositions between the three subgroups, such as those demonstrated below for the tonalitic-trondhjemitic gneiss.

The second group, the *c.* 3050 Ma Qeqertaussaq diorite, consists of a group of dioritic, quartz dioritic and mafic tonalitic enclaves in tonalitic-trondhjemitic grey gneiss. These enclaves all possess the same dis-

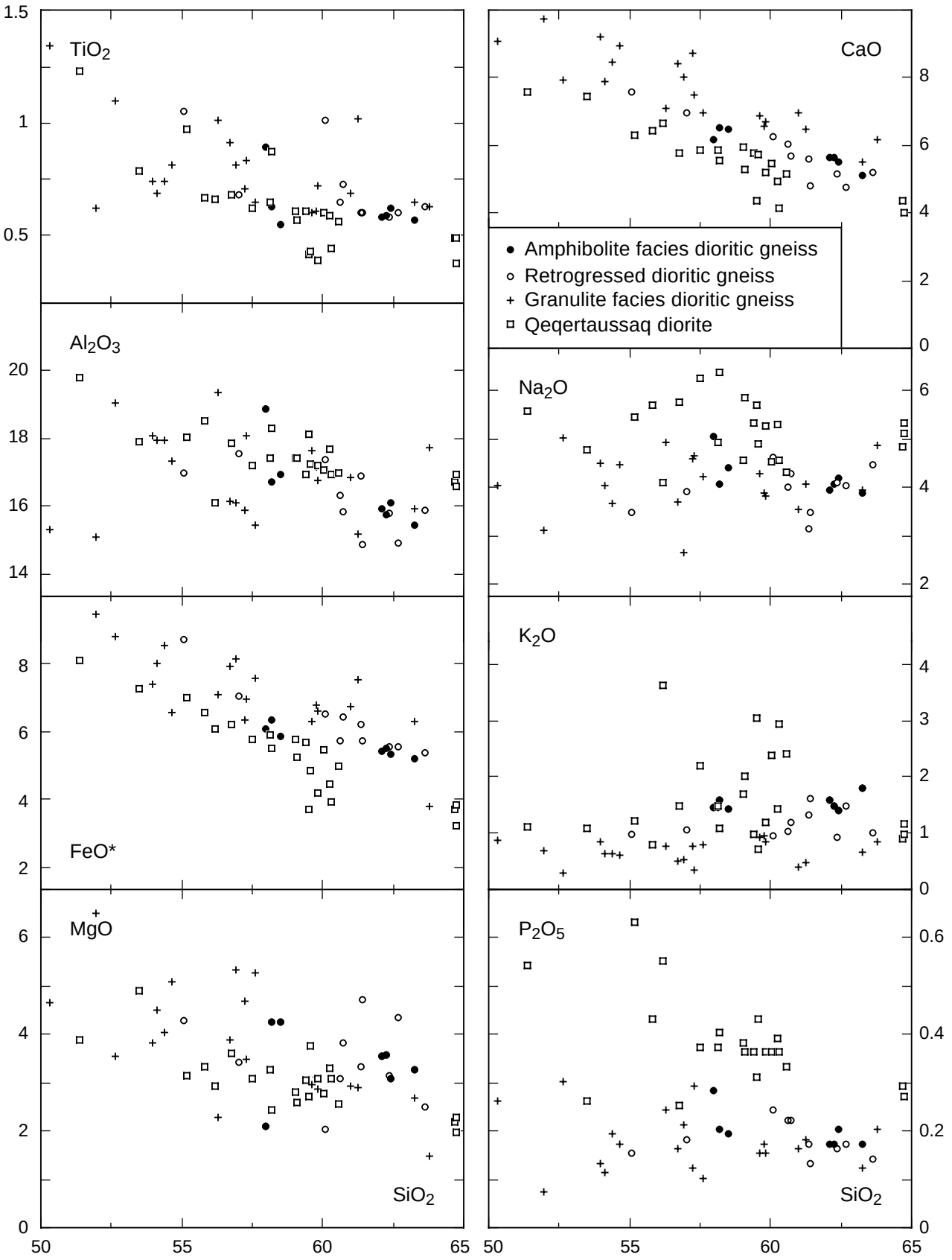

Fig. 55. Major element variation diagrams against SiO_2 (wt. %), dioritic grey gneiss. Note the differences between the main group of dioritic grey gneiss and the Qeqertaussaq diorite. Sample localities in Fig. 52.

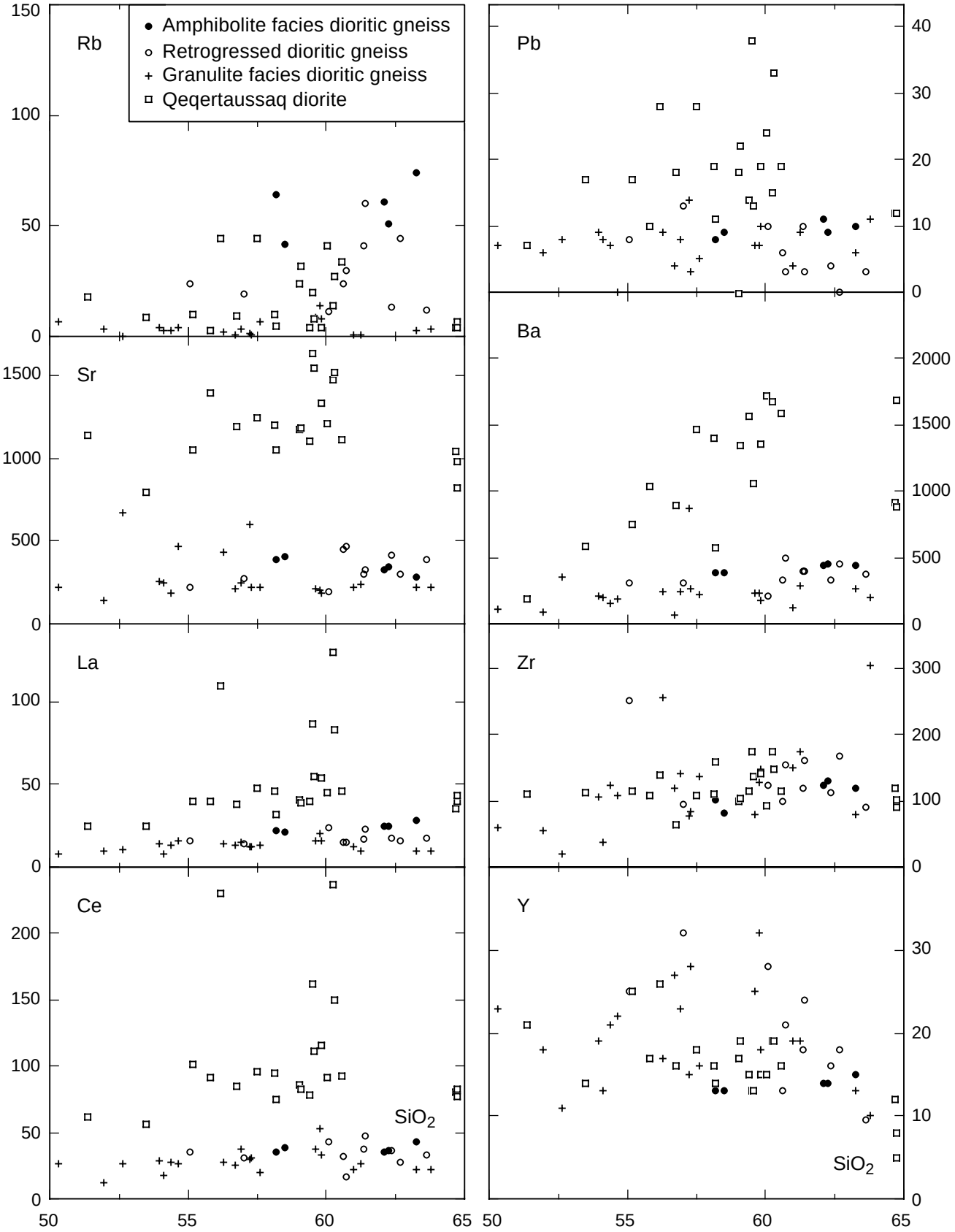

Fig. 56. Selected trace element variation diagrams against SiO_2 (in ppm and wt. %) for dioritic grey gneiss. Note the LIL element and LREE enrichment in the Qeqertaussaq diorite. All elements analysed by XRF (see Appendix for details). Sample localities shown in Fig. 52.

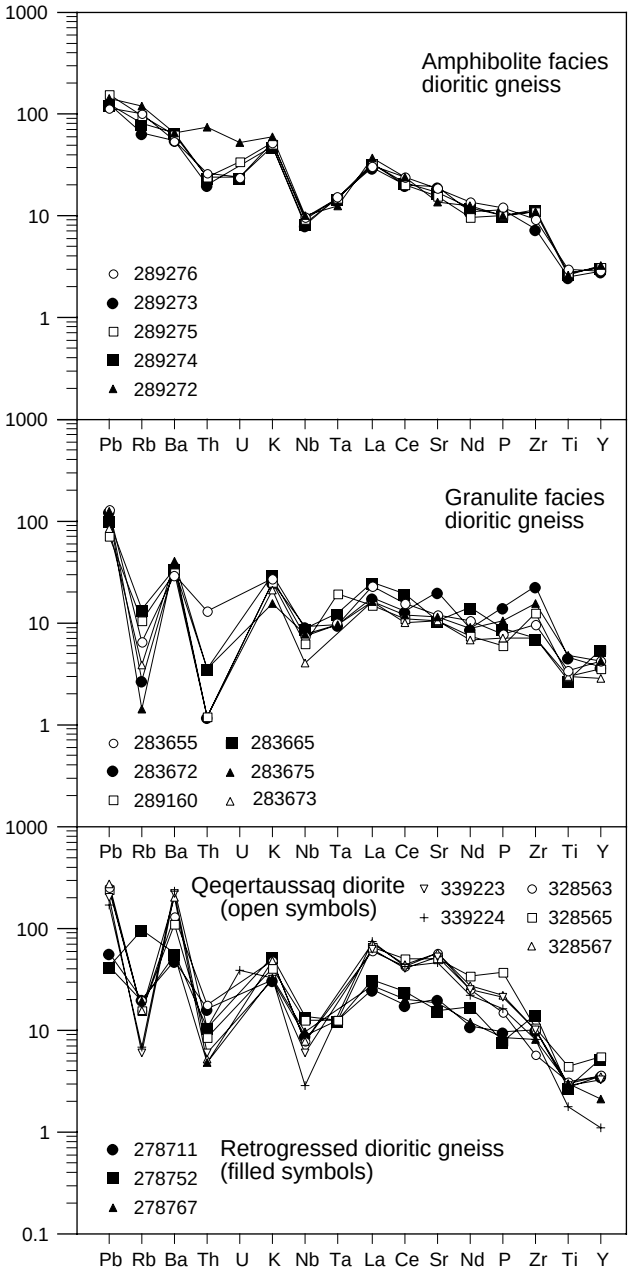

Fig. 57. Spider diagrams of dioritic grey gneiss normalised to primordial mantle, using normalisation factors from Sun & McDonough (1989). XRF and INNA analyses (Th, U, Ta, La, Ce and Nd) in this and succeeding spider diagrams as described in Appendix. Sample localities shown in Fig. 52.

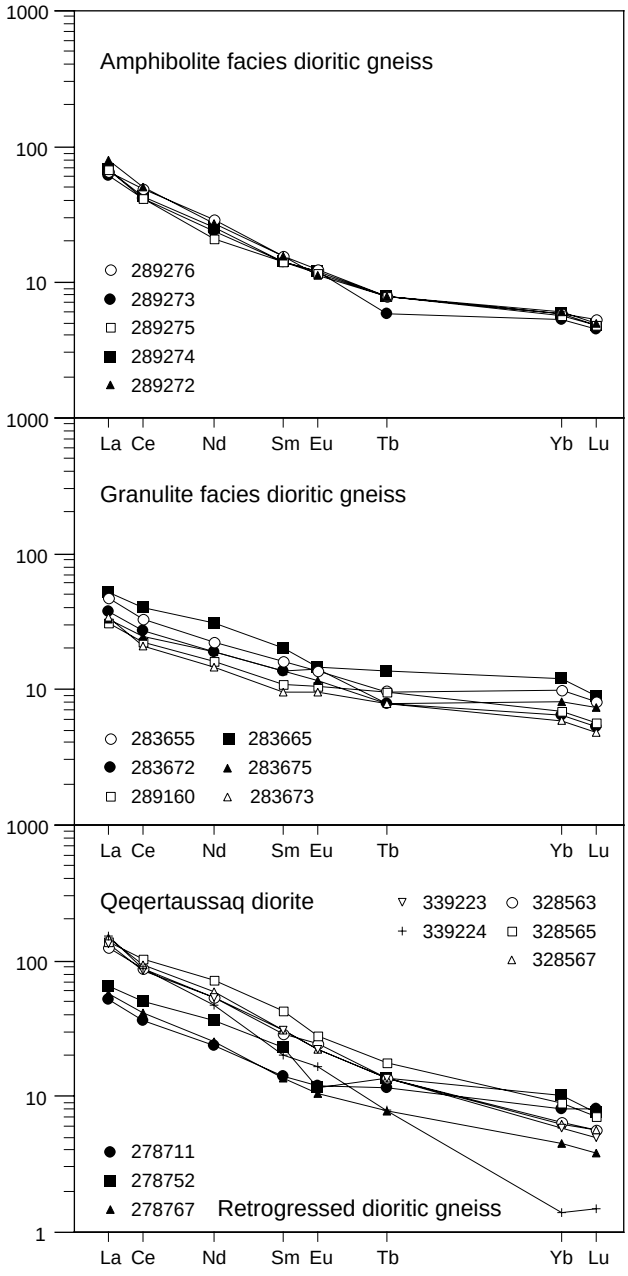

Fig. 58. Chondrite-normalised REE diagrams (Nakamura, 1974) of dioritic grey gneiss from the Fiskefjord area. Note LREE enrichment in the Qeqertaussaq diorite. All elements analysed by INNA (see Appendix). See Fig. 52 for sample localities.

tinct geochemical signature and are located around the peninsula Qeqertaussaq in central Fiskefjord (with a dextral offset of *c.* 3 km across Fiskefjord by the Proterozoic Fiskefjord fault). The Qeqertaussaq diorite is variably retrogressed but may contain partially preserved hypersthene. In the field these rocks are indistinguishable from retrogressed members of the common dioritic gneiss, and likewise form early and commonly fragmented components of the grey gneiss. However, the Qeqertaussaq diorite is clearly geochemically different from the common dioritic gneiss including its retrogressed samples, being enriched in P_2O_5, LREE and several LIL elements but depleted in HFS (high field strength) elements (Appendix 6; Figs 55–58) relative to rocks of the

former unit with similar SiO_2 content. The Qeqertaussaq diorite has low TiO_2, FeO*, MgO, CaO, Cr and Ni contents and low Mg/Fe ratios, whereas it has very high contents of especially P_2O_5, Pb, Ba, Sr and LREE, and relatively high contents of Na_2O, K_2O, Pb, Rb and other LIL trace elements. Zr and Y occur in similar concentrations as found in the common dioritic gneiss. Fig. 58 displays the strong REE fractionation of the Qeqertaussaq diorite and its distinct positive LREE anomaly compared to common dioritic gneiss. The HREE contents of both groups of dioritic gneiss are significantly higher than in the tonalitic-trondhjemitic grey gneiss (compare Figs 58 and 62).

Tonalitic-trondhjemitic grey gneiss

Major and trace element variation diagrams against SiO_2 based on 122 samples (Figs 59, 60), as well as mantle-normalised spider diagrams and chondrite-normalised REE diagrams of representative samples (Figs 61, 62), illustrate the chemical composition and variation of the tonalitic-trondhjemitic gneiss. Sample localities are shown on Fig. 53, and representative compositions and bulk averages are listed in Appendixes 7–8. The figures also highlight compositional differences between amphibolite facies (un-retrogressed) rocks, granulite facies rocks, and retrogressed rocks (also in amphibolite facies, but with disequilibrium mineral textures and compositions).

The major element compositions of the three groups of tonalitic-trondhjemitic gneiss (Appendixes 7, 8) are typical for intermediate to acid rocks of the tonalite-trondhjemite-granodiorite (TTG) suite (see e.g. reviews by Condie, 1981 and Martin, 1994), and plotted against SiO_2 (Fig. 59) most major element oxides only display moderate scatter, suggesting that the rocks may have been formed by similar magmatic processes. However, both Na_2O and K_2O and several LIL trace elements show large variations in the retrogressed gneiss (see below). Besides, Fig. 59 suggests that the granulite facies gneiss group has higher FeO*, MgO and CaO and lower Al_2O_3, Na_2O and K_2O concentrations than the two other groups, and FeO* and MgO appear to be more variable in retrogressed gneiss than in the amphibolite and granulite facies groups.

In order to investigate if these apparent differences between gneisses with different metamorphic facies are statistically significant, covariance tests between the three groups of grey gneiss were performed for all major element oxides against SiO_2 (major elements recalculated to 100%), whereby the silica content of each sample could also be taken into account. The test confirmed that the differences are all significant at the 99% confidence level (F-values above 7.50, critical F_{99} = 4.78), except for TiO_2 and P_2O_5 where there is no significant difference (F-values of 0.80 and 0.74 respectively). A linear relationship between each major element oxide and SiO_2 was assumed in the covariance tests; this is not true for K_2O, but Fig. 59 itself shows that the differences in K_2O are very large.

Amphibolite facies, granulite facies and retrogressed orthogneiss have different LIL trace element compositions, and examples of Rb and Pb are plotted against SiO_2 in Fig. 60. Amphibolite facies gneiss has normal, and granulite facies gneiss very low concentrations of these elements compared to average Archaean TTG from the literature sources quoted above. Retrogressed gneiss has lower LIL element concentrations than amphibolite facies gneiss, but there are large variations irrespective of SiO_2 content. Sr and Ba show different distributions (Fig. 60). Compared to average 'Archaean TTG' (Sr = 454 ppm, Ba = 690 ppm, Martin's, 1994, compilation), the concentrations are normal to low in both amphibolite facies gneiss and granulite facies gneiss (average amphibolite facies: Sr = 382 ppm, Ba = 691 ppm; granulite facies: Sr = 417 ppm, Ba = 430 ppm, Appendix 7). However, in retrogressed gneiss both Sr and Ba concentrations are above average Archaean TTG (average 692 and 809 ppm, respectively, Appendix 8). A few of the latter samples have Sr and Ba concentrations above *c.* 900 and 1500 ppm together with high concentrations of P_2O_5, LREE and other LIL elements (see below); these samples all occur within the area of the Qeqertaussaq diorite and are shown with open squares on Figs 59 and 60. Each of the elements La, Ce, Zr and Y (Fig. 60) is quite variable but occurs within similar limits in the three groups of grey gneiss, except in the just mentioned LREE-enriched samples of retrogressed gneiss.

In mantle-normalised spider diagrams (Fig. 61) all three groups of tonalitic-trondhjemitic gneiss show progressive enrichment from the least to the most incompatible lithophile elements relative to primordial mantle, but with negative deviations from this curve of the HFS elements Nb and to a lesser degree Ta and Ti. In addition, retrogressed and particularly granulite facies gneisses show very substantial negative Rb and Th anomalies. The overall pattern of amphibolite facies gneiss closely resembles that of average Archaean grey gneiss (Fig. 63, using Martin's, 1994, compilation), and is comparable to the patterns of some younger calc-

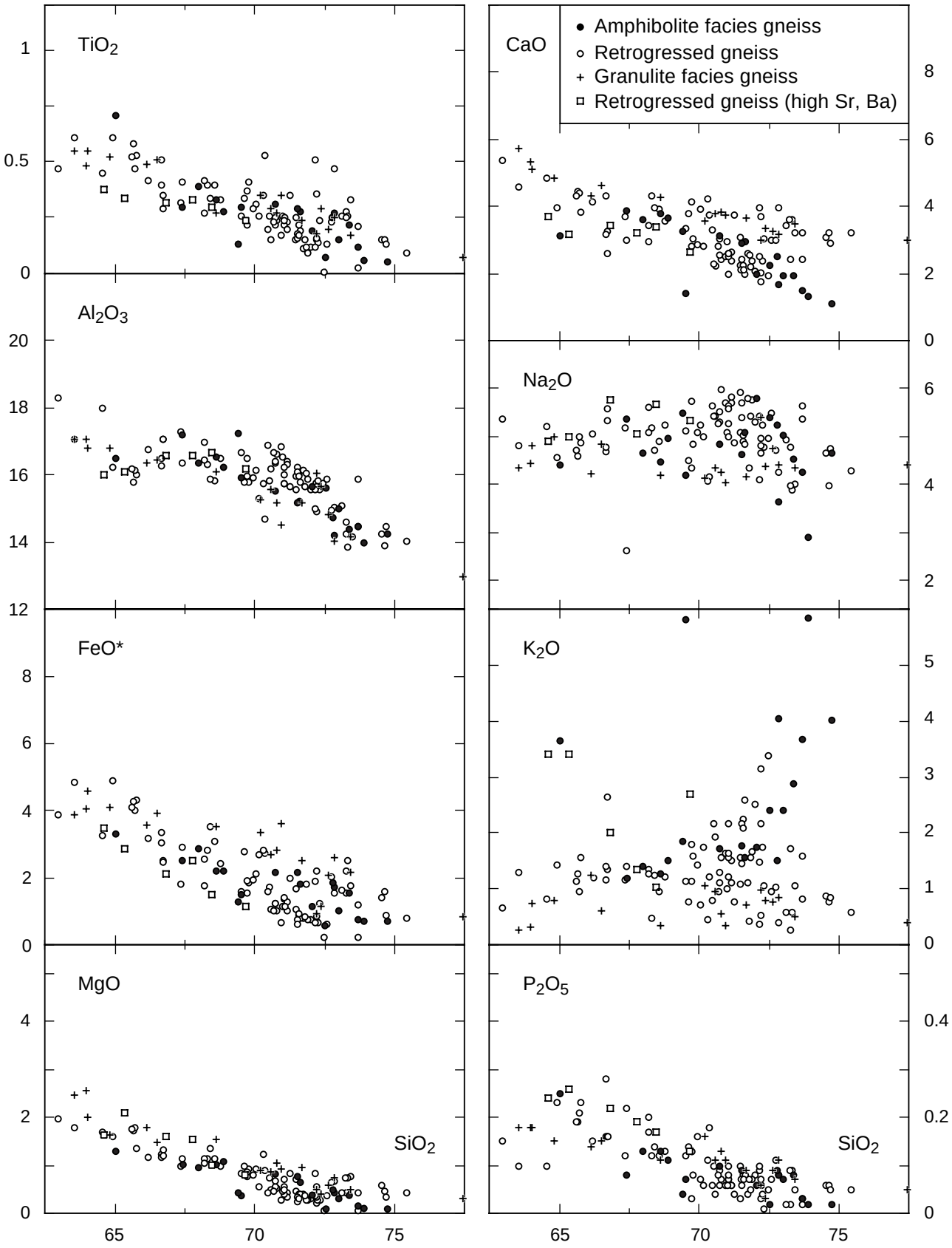

Fig. 59. Major element variation diagrams *v.* SiO_2 (wt. %), tonalitic-trondhjemitic grey gneiss. See Fig. 53 for locations of samples.

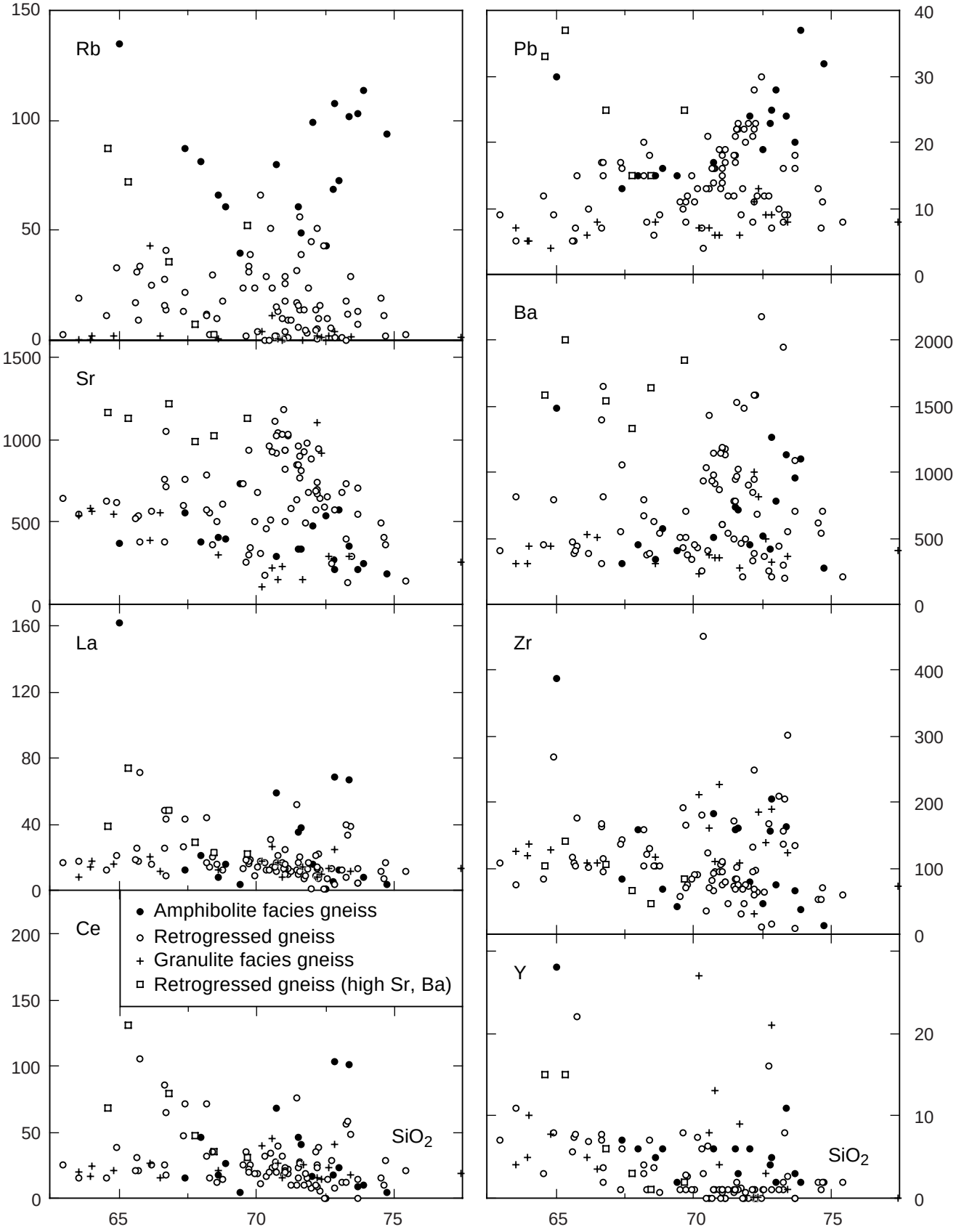

Fig. 60. Selected trace element variation diagrams against SiO_2 (in ppm and wt. %), tonalitic-trondhjemitic grey gneiss. All elements analysed by XRF (see Appendix for details). See Fig. 53 for locations of samples.

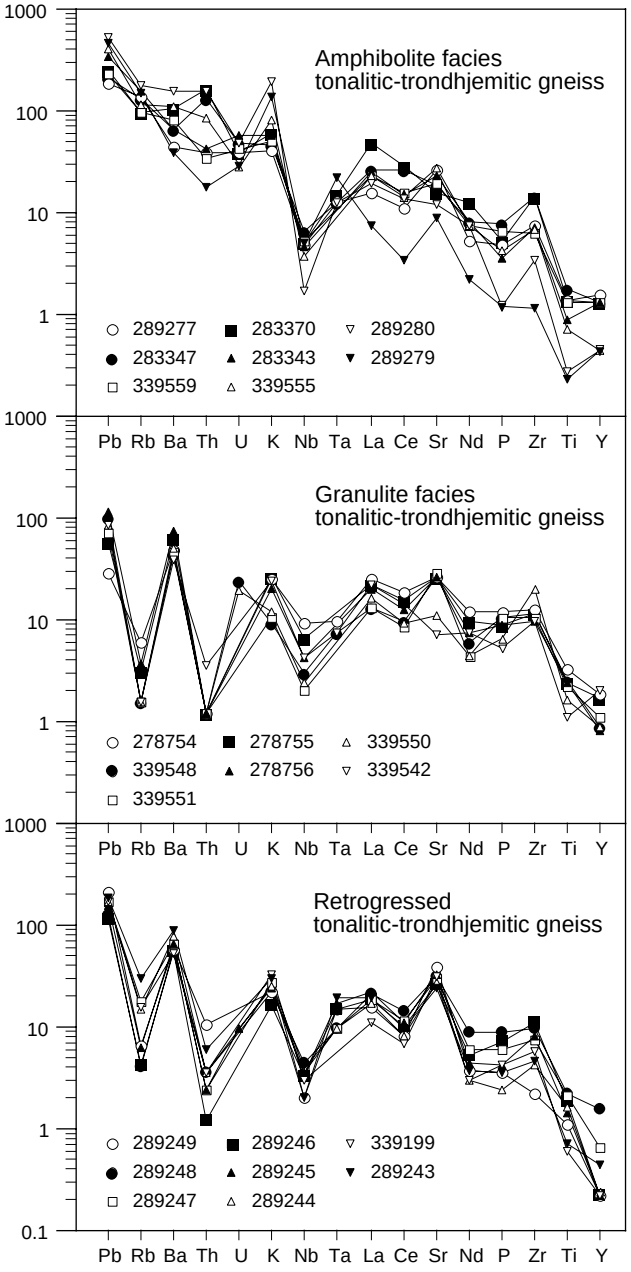

Fig. 61. Spider diagrams of tonalitic-trondhjemitic grey gneiss, Fiskefjord area, normalised to primordial mantle (normalisation factors from Sun & McDonough, 1989). XRF and INNA analyses, see Appendix. See Fig. 53 for locations of samples.

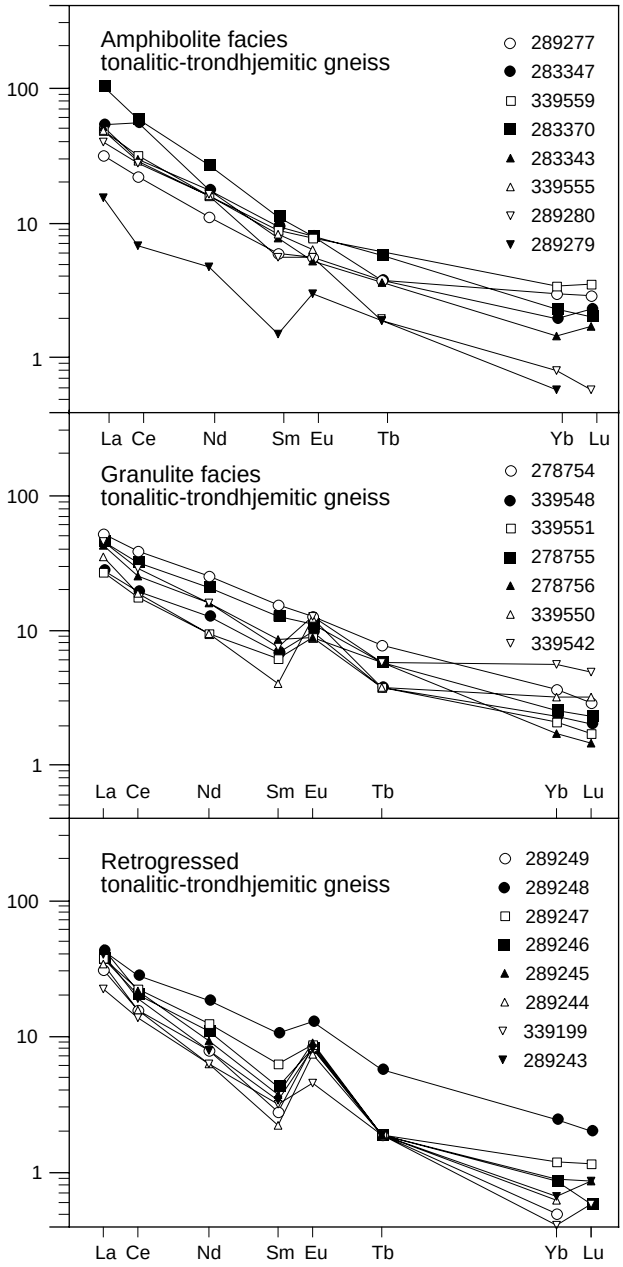

Fig. 62. Chondrite-normalised REE diagrams (Nakamura, 1974) of tonalitic-trondhjemitic grey gneiss, Fiskefjord area. All elements analysed by INNA (see Appendix). Locations of samples in Fig. 53.

alkaline suites (e.g. review by Tarney & Jones, 1994). The spider diagrams from the Fiskefjord area also bring out the low concentrations of all LIL elements in granulite facies gneiss, and show the very variable concentrations of most LIL elements and high concentrations of Sr and Ba in the retrogressed gneiss.

Chondrite-normalised REE diagrams (Fig. 62) show strong fractionation. In all three groups of tonalitic-trondhjemitic gneiss the LREE are strongly enriched, whereas HREE concentrations are close to chondrite values (average LaN/YbN values for amphibolite facies, granulite facies, and retrogressed gneiss are 27.3, 12.8 and 38.9, respectively). Y is also low (Fig. 60); this pattern is typical for most Archaean TTG suites but less common in younger calc-alkaline orogenic granitoids. All analysed samples of retrogressed gneiss have a dis-

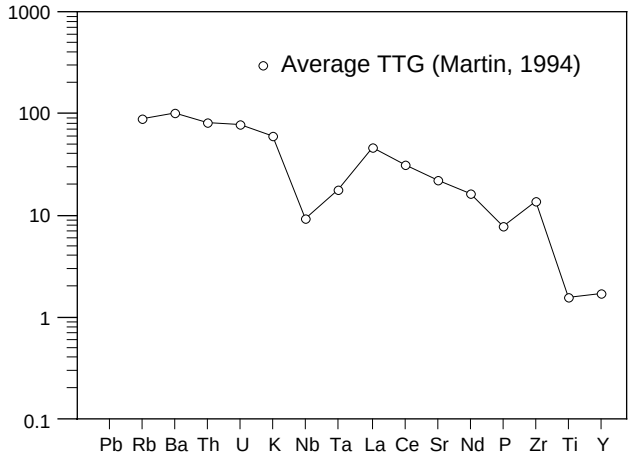

Fig. 63. Mantle-normalised spider diagram of average Archaean TTG (Martin, 1994) for comparison with grey gneiss (Fig. 61) and the Finnefjeld and Taserssuaq complexes (Fig. 71).

tinct positive Eu anomaly, which appears to be less common in the two other groups

Mineral chemistry

Representative microprobe analyses of mafic minerals and feldspars from three metamorphic groups of grey gneiss are shown in Tables 3 and 4, and Table 5 shows similar analyses from the Qugssuk granite. The granite may be considered equivalent to amphibolite facies grey gneiss in terms of the relationships between mineral compositions and metamorphic facies. Systematic variations in the compositions of amphibole and biotite, especially TiO_2, Al^{iv}, Na and K in amphibole, and TiO_2 in biotite, show that retrogression occurred under very variable (amphibolite facies) temperature and pressure

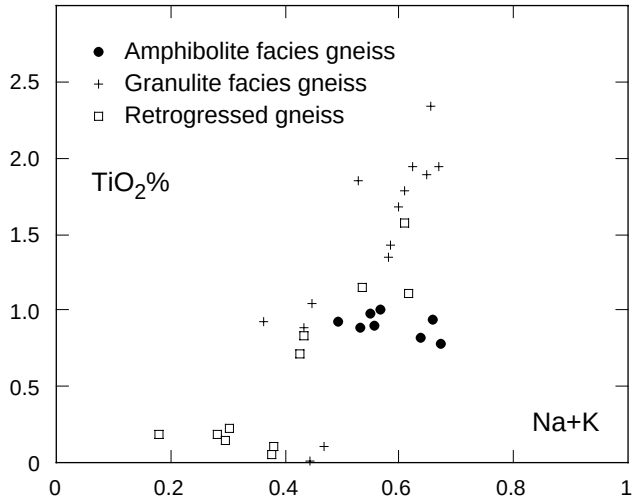

Fig. 64. TiO_2 plotted against Na + K in hornblende and actinolitic hornblende from amphibolite facies, granulite facies, and retrogressed grey gneiss. Amphiboles from retrogressed gneiss have a large range of TiO_2 and Na + K contents, which in part overlap with those of amphibolite and granulite facies hornblendes. The data may suggest two different events of retrogression. See Table 3 for analytical details.

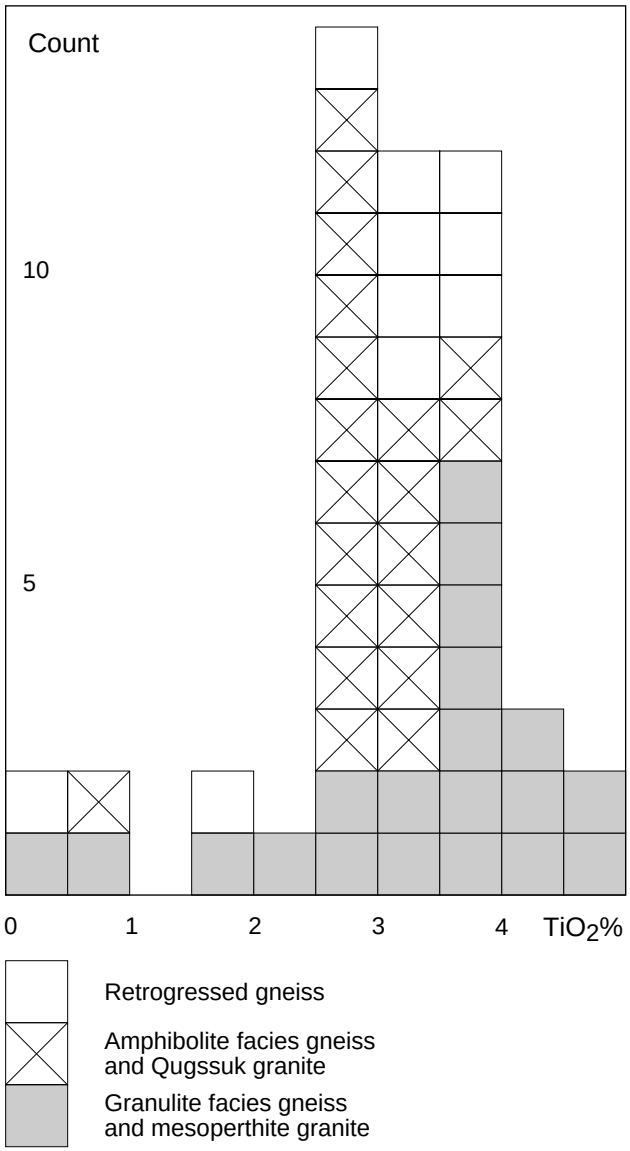

Fig. 65. Distribution of TiO_2 contents in biotites from amphibolite facies grey gneiss and granite, granulite facies grey gneiss and mesoperthite granite, and retrogressed grey gneiss. Note that many biotite grains in retrogressed gneiss have relatively high TiO_2 contents (also these grains being sheaf-like and retrograde), and that amphibolite and granulite facies gneiss may also contain a few biotite grains with very low TiO_2 contents; the latter are small secondary grains which were probably formed during late retrogression. See Table 3 for analytical details.

Table 3. Representative mineral compositions, amphibolite and granulite facies grey gneiss

GGU	Amphibolite facies							Granulite facies										
No	289272	289276	289277	289272	289276	289272	289276	278738	278738	278756	278738	278754	278756	278754	278754	278738	278754	278756
Mineral	bt 7-10	bt 28-36	bt 71-73	hbl 11-12	hbl 18-27	pl 17-18	pl 7-10	bt 25	bts 19-20	bt 11+14	hbl 58-60	hbl 35-38	hbl 19-22	opx 39-42	cpx 43-46	pl 14	pl 31-34	pl 7-10
SiO_2	36.76	36.68	36.14	44.38	44.26	60.13	59.26	35.47	36.46	37.16	43.50	43.40	43.59	52.41	51.97	59.95	60.39	60.91
TiO_2	2.60	3.25	2.67	0.89	1.00	0.01	0.01	3.78	3.01	3.24	1.95	1.89	2.34	0.07	0.19	n.d.	0.12	0.02
Al_2O_3	15.43	15.11	16.61	9.92	10.28	24.04	24.41	15.31	15.44	15.69	10.40	10.07	10.02	0.88	1.86	25.04	24.83	24.43
FeO	18.18	18.55	18.65	16.54	16.69	0.05	0.05	19.09	17.47	17.37	16.45	14.98	15.89	25.76	10.70	0.06	0.08	0.15
MnO	0.27	0.24	0.26	0.38	0.38			0.02	0.11	0.02	0.11	0.17	0.15	0.74	0.37			
MgO	11.98	11.81	10.48	10.52	10.56	0.03	0.03	11.06	13.08	12.18	10.52	11.53	11.04	19.50	12.53	n.d.	0.01	0.09
CaO	0.02	0.02	0.04	11.88	11.99	6.39	6.65	0.08	n.d.	0.08	11.47	11.91	11.76	0.65	22.11	6.36	7.06	6.44
Na_2O	0.25	0.02	0.08	1.11	1.24	8.00	7.45	0.06	0.06	0.02	1.26	1.33	1.43	n.d.	0.61	7.92	7.53	7.62
K_2O	9.39	9.64	9.53	1.08	1.10	0.23	0.23	9.55	9.73	9.35	1.34	1.36	1.27	n.d.	n.d.	0.38	0.49	0.60
Cl	0.03	0.02	0.03					n.d.	n.d.	0.05								
Sum	94.91	95.34	94.49	96.70	97.50	98.88	98.09	94.42	95.36	95.16	97.00	96.64	97.49	100.01	100.34	99.71	100.51	100.26
Ofor Cl	0.01	0.01	0.01					0.00	0.00	0.01								
FeO′				13.65	13.78						13.39	12.80	13.73	25.76	8.47			
Fe_2O_3′				3.21	3.23						3.40	2.42	2.40	0.00	2.48			
Sum′	94.90	95.33	94.48	97.02	97.82			94.42	95.36	95.15	97.34	96.88	97.73	100.01	100.59			
Ba	2000	3000		160	190	120	270	8200	2000	7400	380	340	350	60	115	580	350	590
Sr	n.d.	n.d.		n.d.	n.d.	500	650	n.d.	n.d.	n.d.	n.d.	n.d.	n.d.	n.d.	n.d.	830	630	590
Rb	790	610		n.d.	n.d.	n.d.	n.d.	n.d.	n.d.	190	n.d.	n.d.	n.d.	n.d.	n.d.	n.d.	n.d.	n.d.
Si	2.80	2.79	2.78	6.67	6.60	2.71	2.69	2.74	2.76	2.81	6.52	6.52	6.51	1.99	1.94	2.68	2.68	2.71
Al	1.39	1.36	1.50	1.76	1.81	1.28	1.31	1.39	1.38	1.40	1.84	1.78	1.76	0.04	0.08	1.32	1.30	1.28
Ti	0.15	0.19	0.15	0.10	0.11	0.00	0.00	0.22	0.17	0.18	0.22	0.21	0.26	0.00	0.01	0.00	0.00	0.00
Fe^{2+}	1.16	1.18	1.20	1.71	1.72	0.00	0.00	1.23	1.11	1.10	1.68	1.61	1.71	0.82	0.26	0.00	0.00	0.01
Fe^{3+}				0.37	0.37						0.38	0.27	0.27	0.00	0.07			
Mn	0.02	0.02	0.02	0.05	0.05			0.00	0.01	0.00	0.01	0.02	0.02	0.02	0.01			
Mg	1.36	1.34	1.20	2.35	2.35	0.00	0.00	1.27	1.48	1.37	2.35	2.58	2.46	1.10	0.70	0.00	0.00	0.01
Ca	0.00	0.00	0.00	1.91	1.92	0.31	0.32	0.01	0.00	0.01	1.84	1.92	1.88	0.03	0.88	0.30	0.34	0.31
Na	0.04	0.00	0.01	0.32	0.36	0.70	0.66	0.01	0.01	0.00	0.37	0.39	0.41	0.00	0.04	0.69	0.65	0.66
K	0.91	0.94	0.93	0.21	0.21	0.01	0.01	0.94	0.94	0.90	0.26	0.26	0.24	0.00	0.00	0.02	0.03	0.03
Cl	0.00	0.00	0.00					0.00	0.00	0.01								
Sum	7.83	7.81	7.79	15.44	15.48	5.01	4.99	7.82	7.85	7.76	15.46	15.56	15.54	4.00	4.00	5.01	5.00	5.00
Charge	2.47	2.48	2.39	23	23	8	8	2.37	2.42	2.43	23	23	23	6	6	8	8	8
A+B pos				2.44	2.48						2.46	2.56	2.54					
Or						1.27	1.31									2.14	2.74	3.41
Ab						68.53	66.13									67.79	64.08	65.85
An						30.20	32.56									30.07	33.18	30.74

n.d.=not detected

Locations of samples are shown in Fig. 53. The microprobe analyses were carried out on the Jeol 733 Superprobe at the Geological Institute, University of Copenhagen. For major elements the probe was operated at 15 kV and 15 nA with a slightly defocused beam, using crystal spectrometers for data collection. Natural silicates and oxides of end-member compositions were used as standards, and an on-line ZAF computer programme employed for data reduction. See Table 6 for analytical details regarding Ba, Sr and Rb.

Table 4. Representative mineral compositions, retrogressed grey gneiss

GGU	Retrogressed													
No	278751	278774	278815	289241	289241	278774	278815	289241	278774	289241	278751	278774	278815	289241
Mineral	bt 37	bt 10-11	bt 51-62	bt 57-64	bts 36-39	hbl 14-15	hbl 55-66	hbl 40-47	am 12-13	am 50-56	pl 35	pl 8-9	pl 47-50	pl 65-66
SiO_2	36.65	36.49	36.53	36.63	36.73	44.27	43.58	45.90	45.04	45.93	60.70	61.23	61.70	60.81
TiO_2	3.88	3.28	2.59	1.90	0.47	1.15	1.11	0.06	0.71	0.10	n.d.	n.d.	0.03	0.02
Al_2O_3	16.70	15.60	15.74	16.71	17.04	10.17	10.23	8.97	10.16	9.29	24.75	24.47	23.95	24.04
FeO	17.50	18.20	19.07	17.94	16.60	18.32	19.00	16.50	17.00	16.68	0.06	0.16	0.05	0.10
MnO	0.16	0.14	0.23	0.22	0.17	0.24	0.44	0.42	0.28	0.45				
MgO	10.89	11.56	11.19	11.56	12.73	10.56	9.51	11.54	11.07	11.27	n.d.	n.d.	0.02	0.02
CaO	n.d.	n.d.	n.d.	0.02	0.02	12.01	11.86	11.94	12.20	12.09	6.22	6.06	5.35	6.12
Na_2O	0.03	0.09	0.04	0.05	0.03	1.30	1.35	0.88	0.96	0.87	7.89	8.42	8.58	7.89
K_2O	9.69	9.50	9.65	9.47	9.29	0.87	1.17	0.66	0.81	0.70	0.22	0.54	0.19	0.19
Cl	n.d.	n.d.	0.05	0.08	0.04									
Sum	95.50	94.86	95.09	94.58	93.12	98.89	98.25	96.87	98.23	97.38	99.84	100.88	99.87	99.19
Ofor Cl	0.00	0.00	0.01	0.02	0.01									
FeO′						13.10	15.05	11.01	12.20	11.82				
Fe_2O_3′						5.81	4.40	6.10	5.33	5.40				
Sum′	95.50	94.86	95.08	94.56	93.11	99.47	98.69	97.48	98.76	97.92				
Ba	10300	7460	2800	4180	2130	290	170	140			530	250	170	300
Sr	n.d.	n.d.	n.d.	n.d.	n.d.	n.d.	n.d.	n.d.			610	780	750	1090
Rb	370	80	320	150	n.d.	n.d.	n.d.	n.d.			n.d.	n.d.	n.d.	n.d.
Si	2.76	2.78	2.80	2.79	2.82	6.51	6.52	6.79	6.62	6.78	2.70	2.71	2.74	2.72
Al	1.48	1.40	1.42	1.50	1.54	1.76	1.80	1.56	1.76	1.62	1.30	1.28	1.25	1.27
Ti	0.22	0.19	0.15	0.11	0.03	0.13	0.13	0.01	0.08	0.01	0.00	0.00	0.00	0.00
Fe^{2+}	1.10	1.16	1.22	1.15	1.07	1.61	1.88	1.36	1.50	1.46	0.00	0.01	0.00	0.00
Fe^{3+}						0.64	0.50	0.68	0.59	0.60				
Mn	0.01	0.01	0.02	0.01	0.01	0.03	0.06	0.05	0.04	0.06				
Mg	1.23	1.32	1.28	1.31	1.46	2.32	2.12	2.54	2.43	2.48	0.00	0.00	0.00	0.00
Ca	0.00	0.00	0.00	0.00	0.00	1.89	1.90	1.89	1.92	1.91	0.30	0.29	0.26	0.29
Na	0.00	0.01	0.01	0.01	0.00	0.37	0.39	0.25	0.27	0.25	0.68	0.72	0.74	0.69
K	0.93	0.92	0.94	0.92	0.91	0.16	0.22	0.13	0.15	0.13	0.01	0.03	0.01	0.01
Cl	0.00	0.00	0.01	0.01	0.01									
Sum	7.74	7.80	7.82	7.81	7.84	15.43	15.51	15.27	15.34	15.29	4.99	5.03	5.01	4.99
Charge	2.43	2.40	2.39	2.47	2.45	23	23	23	23	23	8	8	8	8
A+B pos						2.43	2.51	2.27	2.34	2.29				
Or											1.26	2.93	1.07	1.11
Ab											68.79	69.46	73.59	69.19
An											29.95	27.61	25.34	29.70

n.d.=not detected

Locations of samples are shown in Fig. 53. See Tables 3 and 6 for analytical details.

conditions. In Fig. 64 TiO_2 is plotted against Na + K (A position) in amphiboles, and TiO_2 contents of biotites are shown in Fig. 65. Biotite and hornblende in textural equilibrium with hypersthene (in granulite facies gneiss) are the most TiO_2-rich, biotite and hornblende in amphibolite facies gneiss have intermediate TiO_2 contents, and retrograde amphibole and biotite grains (in retrogressed gneiss) have variably intermediate to very low TiO_2 contents. Occasionally two successive phases of retrograde biotite were observed in the same rock, such as in sample 289241 NW of Qugssuk (Fig. 53) where a majority of brown biotite with intermediate TiO_2 contents forms large sheaves, and occasional greenish biotite almost devoid of TiO_2 forms small interstitial flakes (Table 4). A few secondary biotite grains with very low TiO_2 contents have also been found in amphibolite and granulite facies rocks (Fig. 65). Some clearly retrograde, sheaf-like biotite aggregates and spongy amphibole grains have titanium or Al^{iv}-alkali element compositions which overlap with those of biotite and amphibole in amphibolite facies gneiss not retrogressed from granulite facies, suggesting that part of the retrogression in, e.g. sample 289241, took place at intermediate to upper amphibolite facies conditions. However, the large compositional variations of retrograde biotite and amphibole in the retrogressed gneiss

Table 5. Representative mineral compositions, Qugssuk granite

GGU No	278786	278797	278797	278808	278786	278797	278808	278786	278786	278797	278808
Mineral	bt 23-27	bt 62	bts 64-67	bt 99-101	Kfs 31	Kfs 72-73	Kfs 95	pl 29	pl rim32	pl 68-69	pl 96-98
SiO_2	36.88	36.56	37.43	36.90	64.79	64.44	64.39	64.05	68.31	63.45	63.23
TiO_2	2.95	2.78	0.62	3.25	0.07	0.07	0.05	0.05	0.04	n.d.	n.d.
Al_2O_3	16.08	16.87	17.34	17.48	17.81	17.73	18.37	22.95	18.93	23.03	23.09
FeO	18.71	19.65	16.74	18.73	n.d.	0.03	0.05	0.05	n.d.	0.02	0.06
MnO	0.25	0.26	0.21	0.12							
MgO	10.50	10.37	11.87	9.98	n.d.	n.d.	n.d.	n.d.	0.02	n.d.	n.d.
CaO	n.d.	0.04	0.01	n.d.	n.d.	n.d.	n.d.	4.24	0.59	4.68	4.72
Na_2O	0.05	0.04	0.05	n.d.	0.67	0.79	0.60	9.49	11.59	9.13	9.13
K_2O	9.84	10.01	9.63	9.81	15.95	15.76	15.65	0.21	0.10	0.15	0.36
Sum	95.26	96.58	93.90	96.27	99.29	98.82	99.11	101.04	99.58	100.46	100.59
Ba	600	1010	470	1740	2920	4860	7480	n.d.	n.d.	140	120
Sr	n.d.	n.d.	n.d.	n.d.	260	340	530	210	n.d.	240	420
Rb	920	410	390	510	330	130	170	n.d.	n.d.	n.d.	n.d.
Si	2.81	2.76	2.85	2.77	3.01	3.01	3.00	2.81	3.00	2.80	2.79
Al	1.44	1.50	1.56	1.55	0.98	0.98	1.01	1.18	0.98	1.20	1.20
Ti	0.17	0.16	0.04	0.18	0.00	0.00	0.00	0.00	0.00	0.00	0.00
Fe^{2+}	1.19	1.24	1.07	1.18	0.00	0.00	0.00	0.00	0.00	0.00	0.00
Fe^{3+}											
Mn	0.02	0.02	0.01	0.01							
Mg	1.19	1.17	1.35	1.12	0.00	0.00	0.00	0.00	0.00	0.00	0.00
Ca	0.00	0.00	0.00	0.00	0.00	0.00	0.00	0.20	0.03	0.22	0.22
Na	0.01	0.01	0.01	0.00	0.06	0.07	0.05	0.81	0.99	0.78	0.78
K	0.96	0.96	0.93	0.94	0.95	0.94	0.93	0.01	0.01	0.01	0.02
Sum	7.78	7.82	7.81	7.74	5.00	5.00	4.99	5.01	5.00	5.00	5.01
Charge	2.41	2.43	2.41	2.44	8	8	8	8	8	8	8
A+B pos											
Or					94.00	92.92	94.49	1.15	0.55	0.84	1.98
Ab					6.01	7.08	5.51	79.28	96.73	77.29	76.25
An					0.00	0.00	0.00	19.56	2.72	21.88	21.77

n.d.=not detected

Sample locations shown in Fig. 68. See Tables 3 and 6 for analytical details.

may suggest prolonged retrogression during a long period of cooling, or that more than one episode of retrogression took place, as is also indicated by the presence of small biotite grains with low TiO_2 contents in amphibolite and granulite facies gneiss.

Table 6 summarises microprobe analyses of Ba, Sr and Rb and TiO_2 in various minerals from the three metamorphic groups of grey gneiss and a sample of Qugssuk granite. Insofar as Ba, Sr and Rb do not form their own mineral phases in the grey gneiss or granite, their absolute concentrations in the analysed minerals are obviously related to whole rock compositions. More importantly the analyses provide information about Ba, Sr and Rb distributions between coexisting minerals and the different metamorphic groups. Ba preferentially occurs in K-feldspar (*c.* 3000–12000 ppm), but also in biotite (*c.* 2000–8000 ppm); amphibole and plagioclase may contain up to *c.* 600 ppm Ba. Sr is located in feldspars (300–1100 ppm); the Sr content of plagioclase is approximately similar in the three facies groups. Rb preferentially occurs in biotite (up to *c.* 900 ppm in amphibolite facies biotite of grey gneiss and Qugssuk granite, 150 ppm in retrograde biotite), but is notably below the detection limit of 70 ppm in granulite facies, high-titanium biotite, and also low in late secondary biotite grains (sample 289241).

Mineral reactions and movement of granitic melts or fluids during prograde and retrograde metamorphic events are prone to have affected the distributions of Ba, Sr and Rb in different ways. As shown above Ba and Rb are especially accommodated in biotite and K-feldspar (although in different proportions). Prograde

Table 6. Ba, Sr, Rb and TiO_2 contents of minerals from orthogneisses in different metamorphic facies and Qugssuk granite

		Ba ppm	Sr ppm	Rb ppm	TiO_2%
Detection limit (microprobe)		45	100	70	0.01
Amphibolite facies orthogneiss					
289272	Whole rock	444	286	74	0.57
	Biotite	2000	n.d.	790	2.60
	K-feldspar	12100	440	175	
	Plagioclase	120	500	n.d.	
	Hornblende	160	n.d.	n.d.	0.89
Granulite facies orthogneiss					
278738	Whole rock	444	568	2	0.55
	Biotite	8200	n.d.	n.d.	3.78
	Biotite (late)	2000	n.d.	n.d.	3.01
	Plagioclase	580	830	n.d.	
	Hornblende	380	n.d.	n.d.	1.95
Retrogressed orthogneiss					
278774	Whole rock	811	549	19	0.61
	Biotite	7300	n.d.	80	3.28
	Plagioclase	250	780	n.d.	
	Hornblende	290	n.d.	n.d.	1.15
289241	Whole rock	383	668	1	0.36
	Biotite	4180	n.d.	150	1.90
	Biotite (late)	2130	n.d.	n.d.	0.47
	Plagioclase	300	1090	n.d.	
	Hornblende	140	n.d.	n.d.	0.06
Qugssuk granite					
278786	Whole rock	777	146	135	0.10
	Biotite	600	n.d.	920	2.95
	K-feldspar	2920	260	330	
	Plagioclase	n.d.	210	n.d.	

n.d.=not detected

See discussion in the main text.
Analytical procedure: Ba, Sr and Rb were analysed with the instrument described in the text to Table 3, operated at 25 kV with a beam current of 300 nA, beam diameter *c.* 40 µ. In order to minimise volatilisation due to the high beam current and long counting times necessary for sufficient signal intensity, an automatic step procedure was employed during the measurement. Each figure quoted for Ba, Sr or Rb is averaged from one or a few groups of six measurements, each consisting of four adjacent points, and representing total counting times of 240 and 480 seconds at peak and background positions. Under these analytical conditions the calculated lower limits of detection were 45, 100, and 70 ppm (2σ) for Ba, Sr and Rb, respectively. Baryte, strontianite, and rubidium chloride were used as standards, with ZAF corrections as above. A silica glass standard was used as blank for Sr and Rb. Ba contents were empirically corrected for interference by Ti-Kα, where 1% TiO_2 gave an apparent concentration of 40 ppm BaO. Microprobe measurements on leucite and sanidine from Italy using similar analytical conditions agree well with PIXE measurements using separates of the same minerals (J. Rønsbo, personal communication, 1989).

granulite facies metamorphism with partial melting, consumption of K-feldspar and removal of a melt fraction can therefore be expected to have strongly influenced the Ba and Rb contents of remaining biotite (see p. 79). Plagioclase accommodates most of the Sr; mobility of Sr during prograde and retrograde metamorphism must therefore have been linked with recrystallisation of plagioclase.

Element distribution within retrogressed tonalitic-trondhjemitic gneiss in the central and northern parts of the Fiskefjord area

The observations that (a) the major element compositions of amphibolite facies, granulite facies, and retrogressed tonalitic-trondhjemitic gneiss are statistically different, (b) the dioritic grey gneiss comprises a geochemically and geographically distinct group with (amongst other characteristics) very high Sr and Ba contents around the peninsula Qeqertaussaq in central Fiskefjord, and (c) both Sr and Ba are among the most variable elements in the retrogressed tonalitic-trondhjemitic gneiss, together raise the questions as to whether the latter group was originally a geochemically homogeneous population, and hence which elements were actually affected by metasomatism during granulite facies and retrogressive metamorphic events.

The retrogressed gneiss is located in a wide intermediate zone between granulite facies and amphibolite facies areas and might therefore be expected to show geochemical variation of mobile elements that are related to sample location. This problem is difficult to handle with statistical methods alone, but can be addressed with element distribution maps; however, the stream sediment survey from this region undertaken by Steenfelt (1988) was not applicable due to low sample density and because the stream sediments include all rock types within their catchment areas.

Distribution maps of selected elements, based on rock samples of retrogressed gneiss from the northern part of the Fiskefjord area, are presented in Figs 66 and 67. Although the samples are not evenly distributed they provide a visual estimate of variations in the concentrations of the chosen elements. For each element three levels of concentration are shown, each comprising approximately one third of the samples (oxide concentrations of major elements have been retained to facilitate comparison with tables and variation diagrams).

Figure 66 shows geographical distributions of elements in the retrogressed tonalitic-trondhjemitic gneiss,

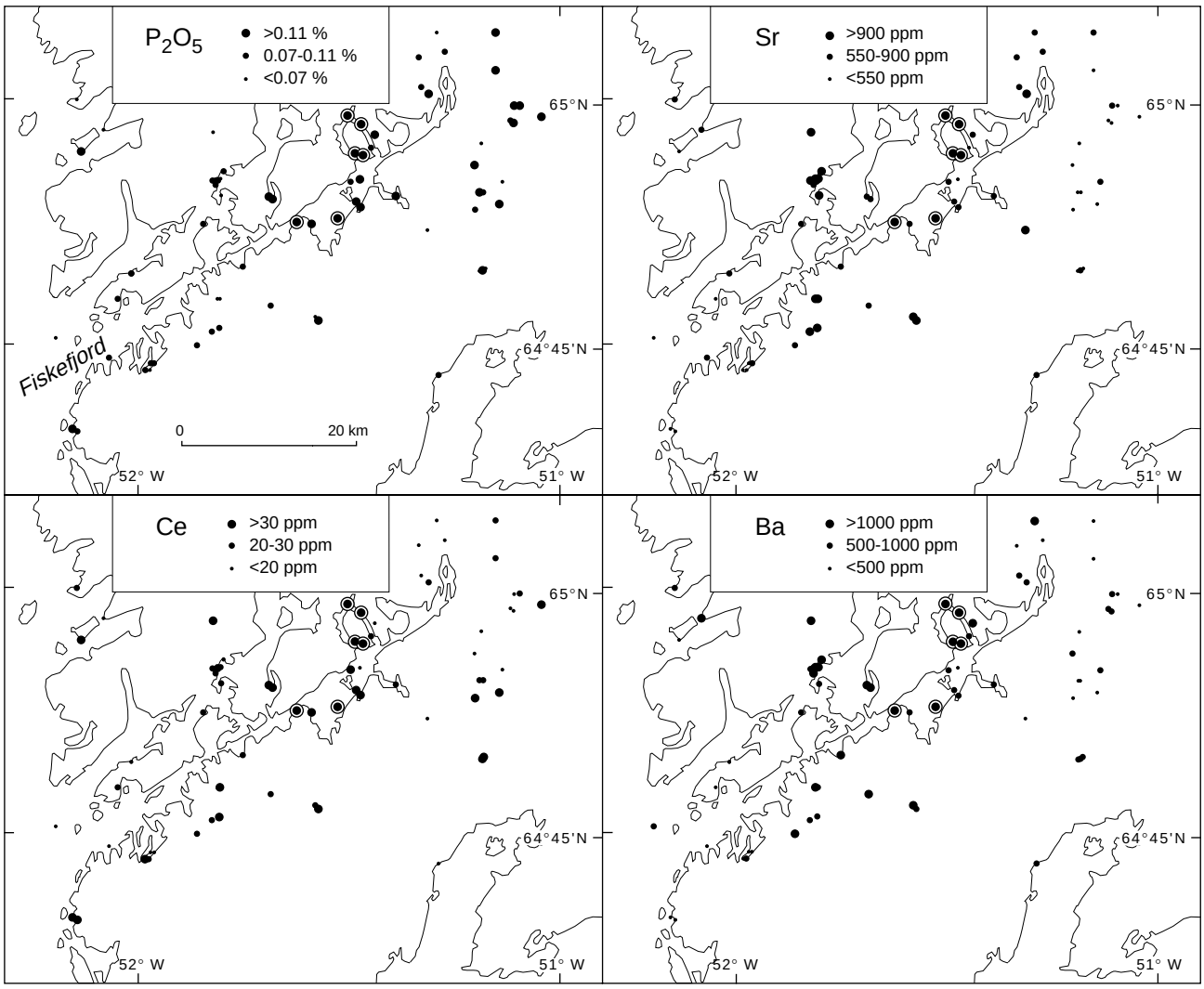

Fig. 66. Distributions of P_2O_5, Sr, Ba and Ce in rock samples of retrogressed tonalitic-trondhjemitic gneiss in the central and northern parts of the Fiskefjord area (oxide concentrations of major elements have been retained to facilitate comparison with tables and other figures). Enrichment of all four elements only occurs within the area of the Qeqertaussaq diorite (ringed samples), suggesting a genetic relationship rather than metamorphic effects in this area; see the main text for further discussion.

which are all strongly enriched in the Qeqertaussaq diorite. Only a few samples have high contents of all four elements (ringed, Fig. 66), all of which occur in the Qeqertaussaq area. Several high values of Sr and Ba also occur south of central Fiskefjord. Figure 67 shows the distributions of LIL elements which are all strongly depleted in granulite facies grey gneiss and very variable in retrogressed grey gneiss – although mostly significantly lower than in the adjacent amphibolite facies gneiss to the east (Appendixes 7, 8). Also these elements are relatively enriched in the samples correlated with the Qeqertaussaq diorite (ringed, Fig. 67). K and Rb, which display fairly similar patterns, are also high in the eastern part of the area, whereas Th has an erratic distribution. The Pb distribution resembles those of Sr and Ba (Fig. 66).

In summary, element distributions in retrogressed tonalitic-trondhjemitic gneiss around Fiskefjord suggest that a few samples in the Qeqertaussaq area, and only there, are geochemically related to the Qeqertaussaq diorite by virtue of a combination of high P, LREE, Sr, Ba, Pb, Rb and K. Moreover, Sr, Ba and Pb (and to some extent K) are concentrated in the central part of the area where retrogression is mostly pervasive. Rb and to some extent K increase eastward towards the area of amphibolite facies gneiss not affected by retrogression, whereas Th is erratic.

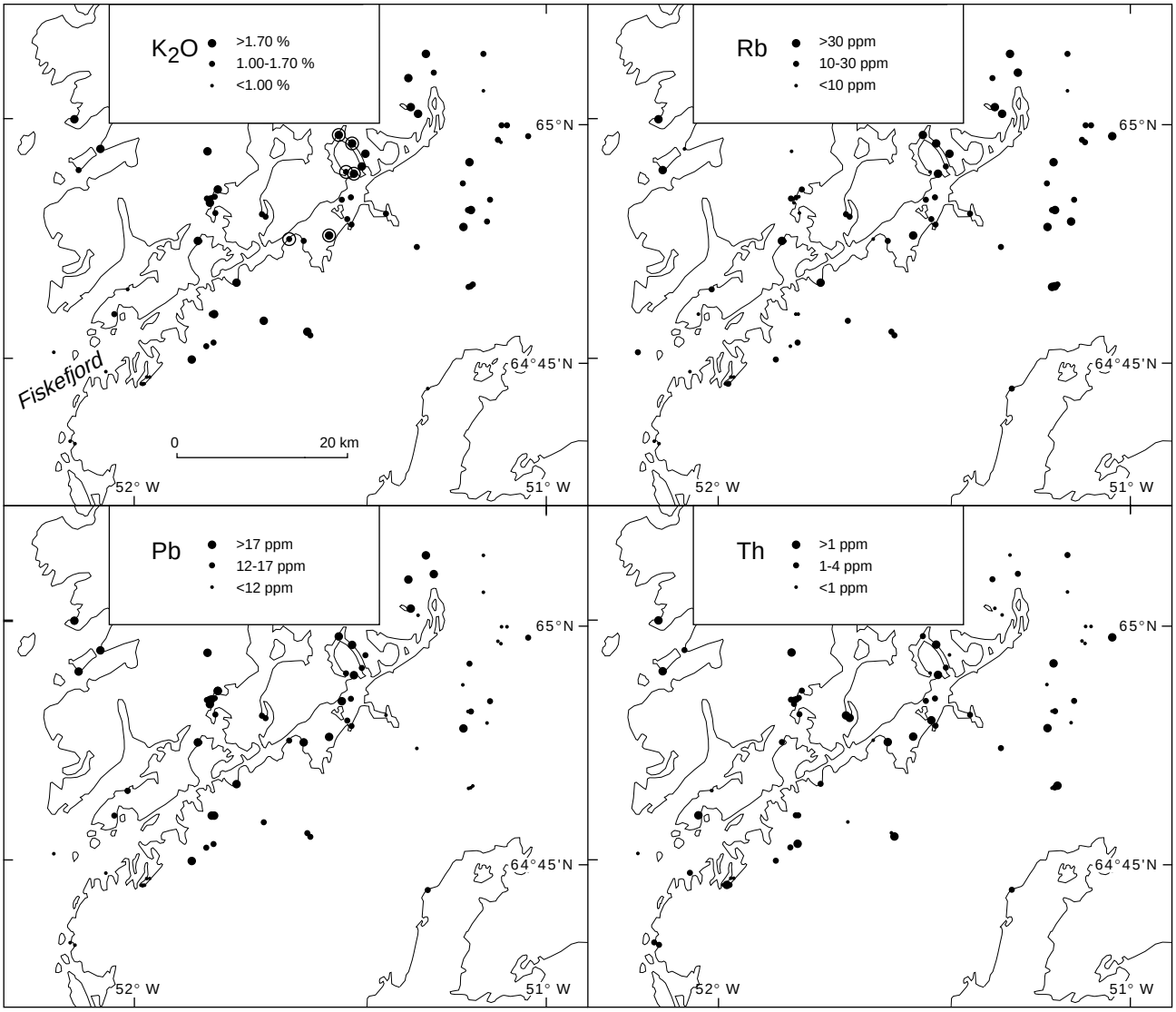

Fig. 67. Distributions of K_2O, Rb, Pb and Th in rock samples of retrogressed tonalitic-trondhjemitic gneiss in the central and northern parts of the Fiskefjord area. See discussion in the main text.

Finnefjeld gneiss and Taserssuaq tonalite complexes

The compositions of available samples from the southeastern parts of the Finnefjeld and Taserssuaq complexes, respectively (sample localities shown on Fig. 68), both largely resemble those of amphibolite facies grey gneiss (Appendix 9; Figs 69, 70). However, the compositions of available samples indicate some general differences between the two complexes. The variation trends of TiO_2, MgO and FeO against SiO_2 appear to be steeper for the Finnefjeld gneiss than for the Taserssuaq tonalite complex, whereas the opposite is the case for Al_2O_3 and CaO. In addition, the Taserssuaq tonalite complex comprises a relatively large granodioritic to granitic group and only a few trondhjemites, whereas the Finnefjeld gneiss complex mainly shows a trondhjemitic trend above 70% SiO_2. These features indicate that partial melting or crystal fractionation processes in the source regions of the two complexes were not identical; a possible interpretation is that plagioclase fractionation was more important in the evolution of the Taserssuaq tonalite than in in the case of the Finnefjeld gneiss complex (see p. 73).

Both complexes have somewhat variable trace element compositions, with increasing LIL element concentrations in the most acid rocks. The concentrations of LIL elements are never as low as in granulite facies

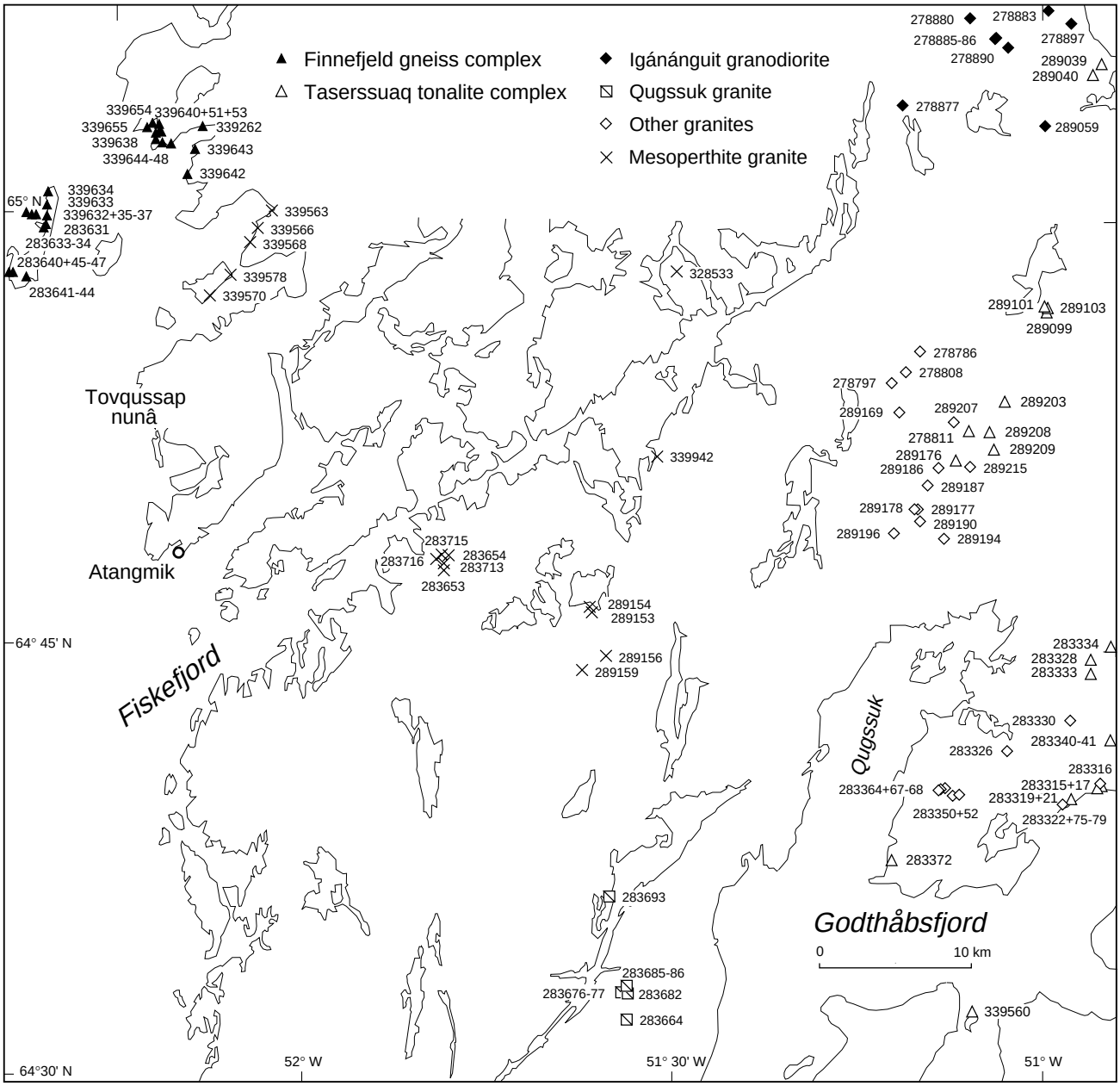

Fig. 68. Locations of analysed samples, Finnefjeld gneiss complex, Taserssuaq tonalite complex and granitic rocks. Five additional samples from the Taserssuaq tonalite complex were collected east of the map area.

grey gneiss, and the very high concentrations of e.g. Sr and Ba encountered in the retrogressed grey gneiss are only approached in a few samples.

Plotted on mantle-normalised spider diagrams (Fig. 71), representative samples from both complexes define clear patterns which are similar to 'average Archaean TTG' (Fig. 63) in general, and to Fiskefjord amphibolite facies grey gneiss in particular (Fig. 61). The patterns are fairly smooth, with high proportions and relatively small variations of the mobile incompatible (LIL) elements, and with clear negative Nb, Ta and Ti anomalies; however, Th and U are depleted in the Finnefjeld gneiss. Sample no. 289208 of Taserssuaq tonalite has very erratic concentrations of incompatible immobile elements and is very high in LIL elements, presumably due to metasomatism.

Also the REE patterns (Fig. 72) are comparable to those of amphibolite facies grey gneiss, with LREE enrichment, strongly fractionated curves, and some samples showing a positive Eu anomaly. Figs 71 and

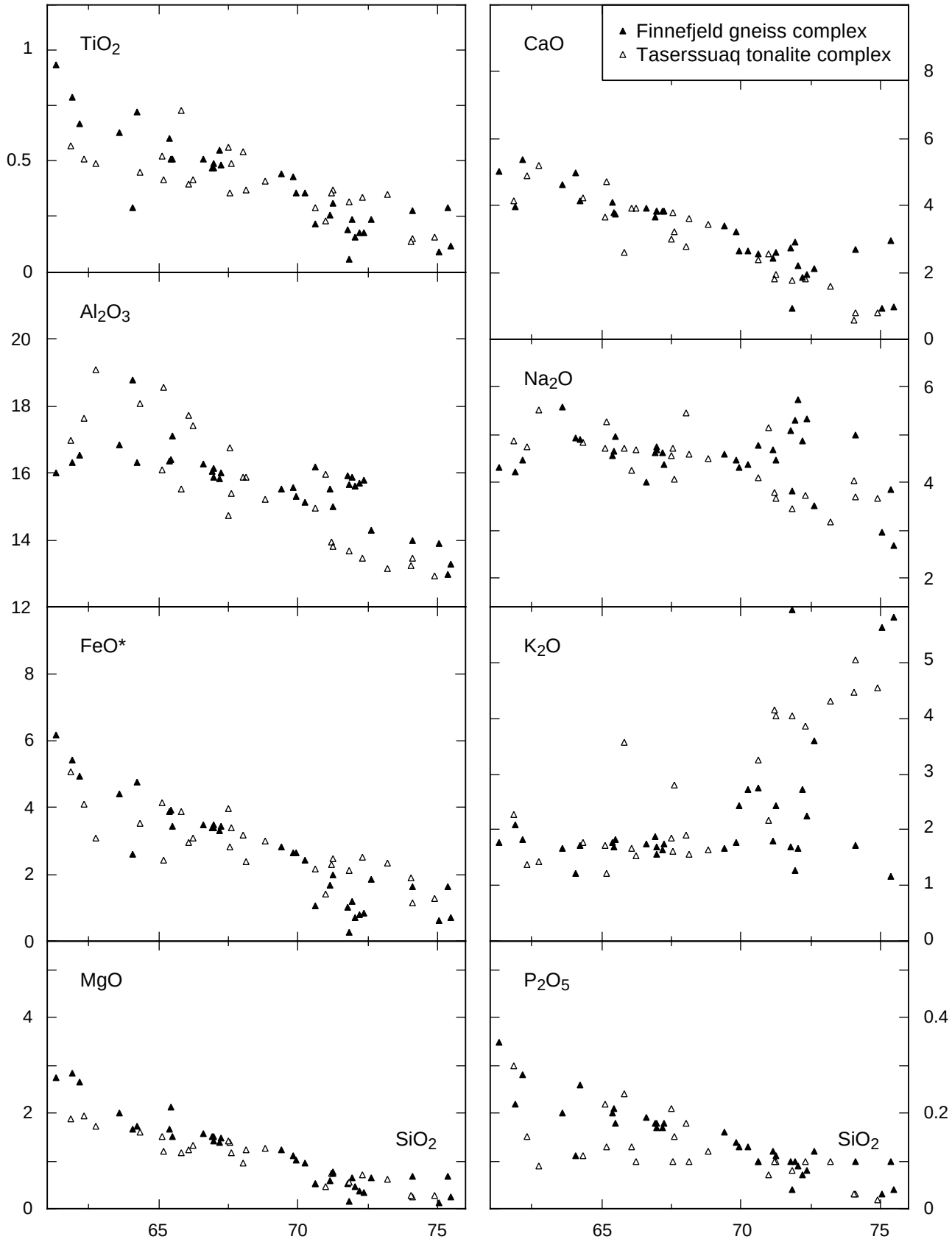

Fig. 69. Major element variation diagrams against SiO_2 (wt. %), Finnefjeld gneiss and Taserssuaq tonalite complexes, Fiskefjord area. See Appendix for analytical details. Sample localities shown in Fig. 68.

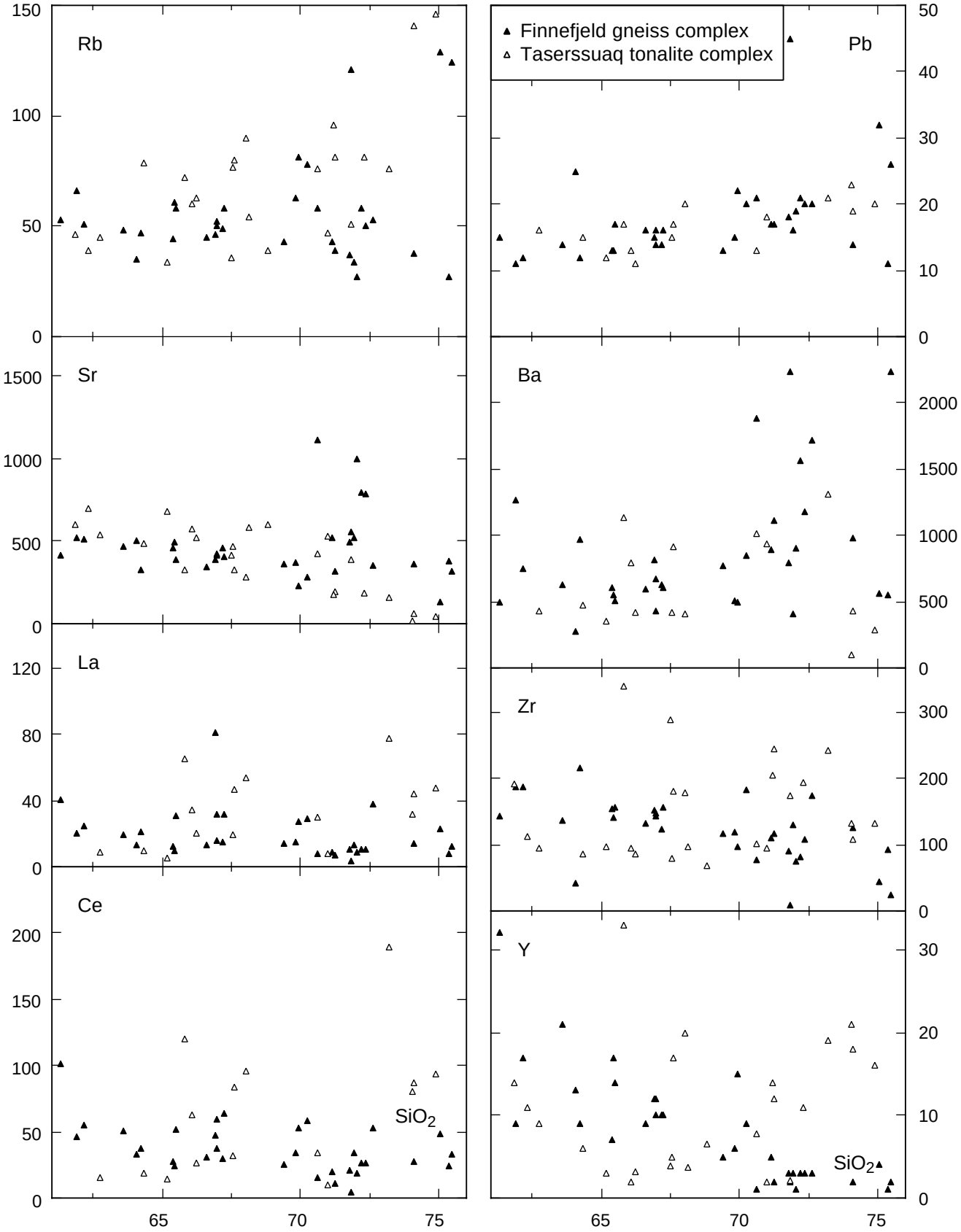

Fig. 70. Selected trace element variation diagrams against SiO_2 (in ppm and wt. %), Finnefjeld gneiss and Taserssuaq tonalite complexes. Analytical details in Appendix. Sample localities shown in Fig. 68.

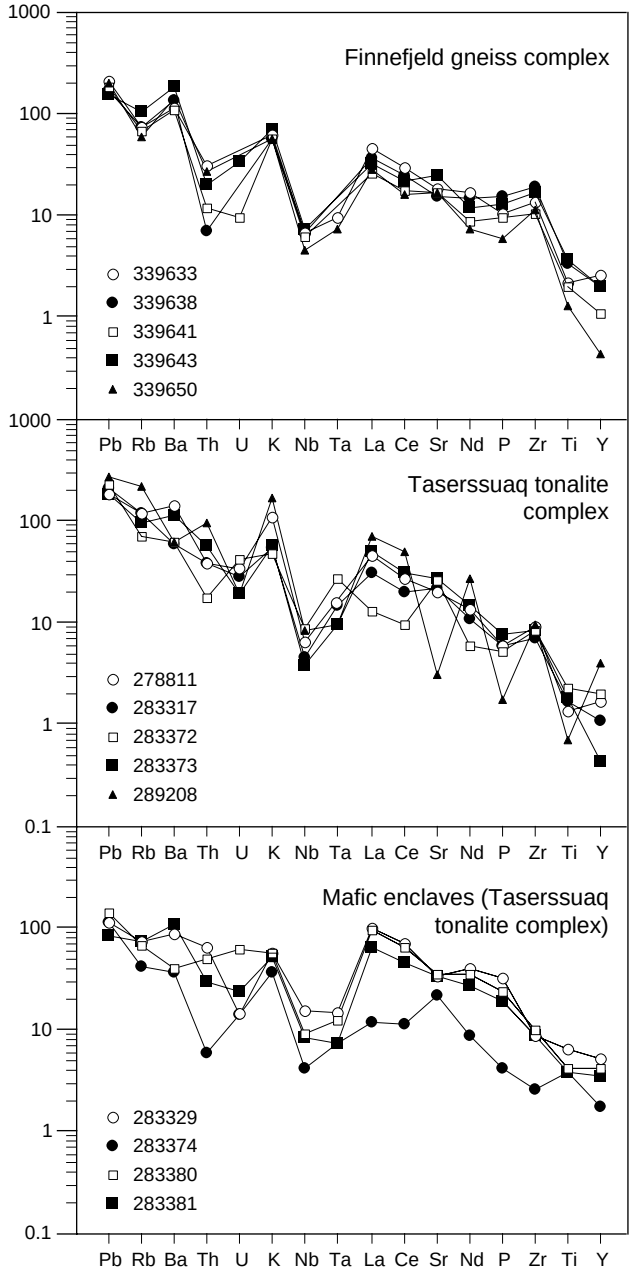

Fig. 71. Spider diagrams of Finnefjeld gneiss and Taserssuaq tonalite complexes, Fiskefjord area, normalised to primordial mantle (Sun & McDonough, 1989). XRF and INNA analyses, see Appendix. Sample localities shown in Fig. 68.

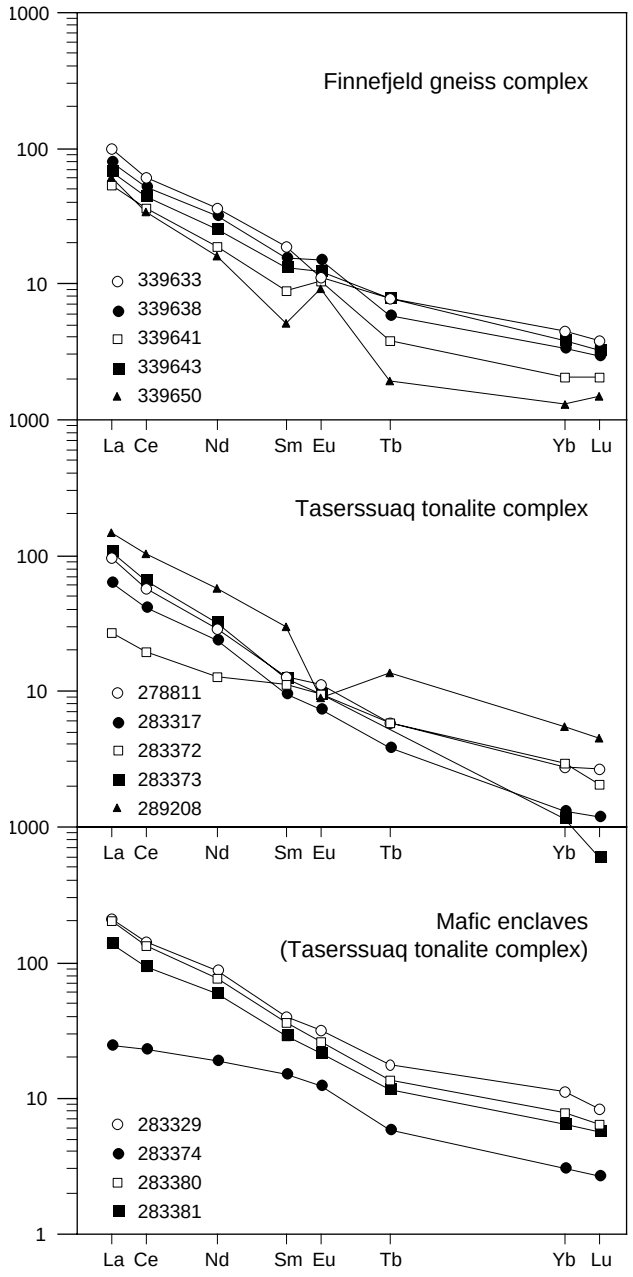

Fig. 72. Chondrite-normalised REE diagrams (Nakamura, 1974) of Finnefjeld gneiss and Taserssuaq tonalite complexes, Fiskefjord area. All elements analysed by INNA (see Appendix). Sample localities shown in Fig. 68.

72 include four hornblende- and plagioclase-rich dioritic to gabbroic enclaves collected in the southern part of the Taserssuaq tonalite complex (analyses in Appendix 9). The multi-element patterns of three of these samples resemble those of the Taserssuaq tonalite complex, except that they have higher REE and Y contents and slightly less fractionated REE spectra than the tonalite complex itself. Sample 283374 has an altogether different composition and lower REE contents combined with weak REE fractionation; it therefore appears not to be related to the complex and could be of supracrustal origin.

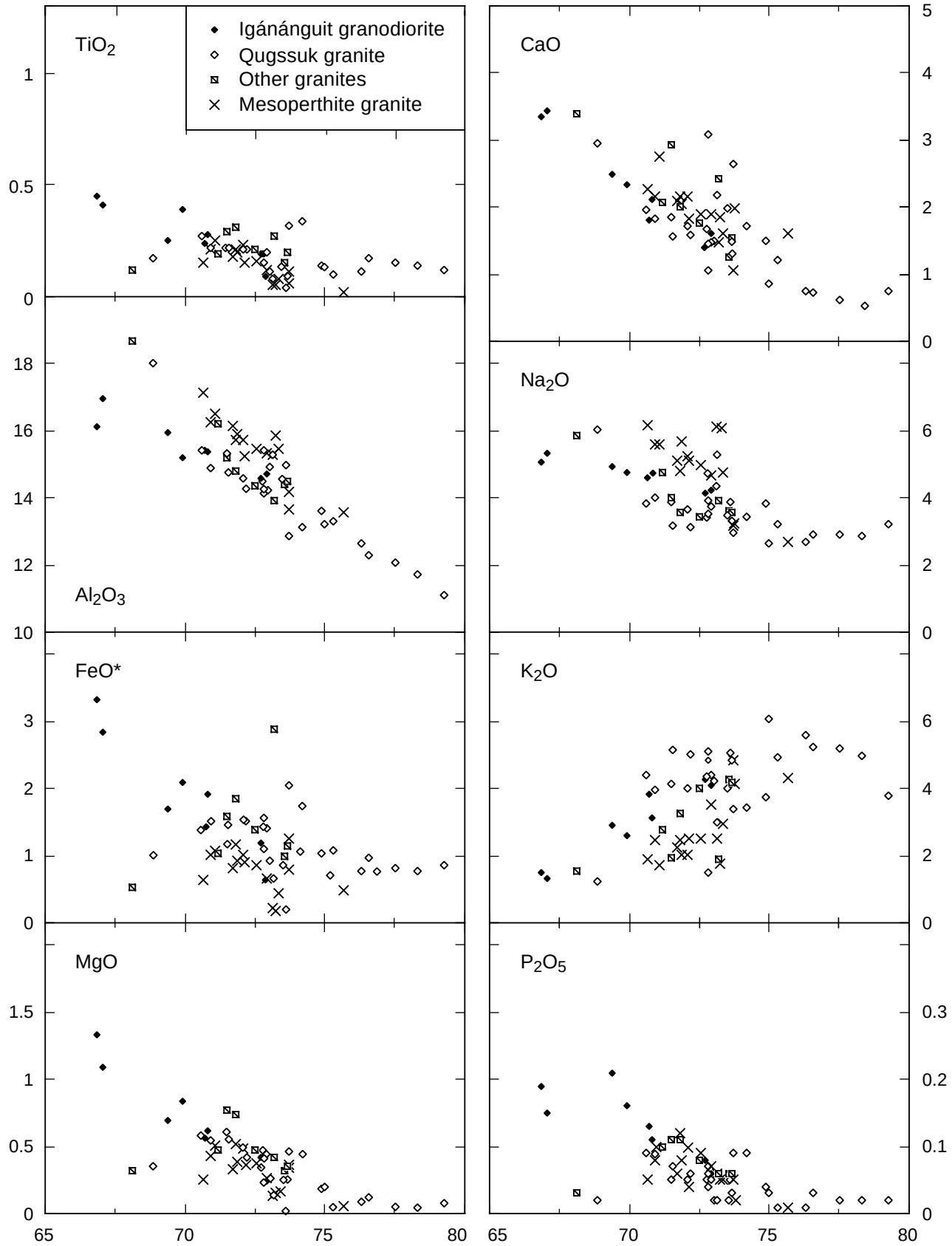

Fig. 73. Major element variation diagrams against SiO_2 (wt. %), granitic rocks, Fiskefjord area. See Appendix for analytical details. Sample localities shown in Fig. 68.

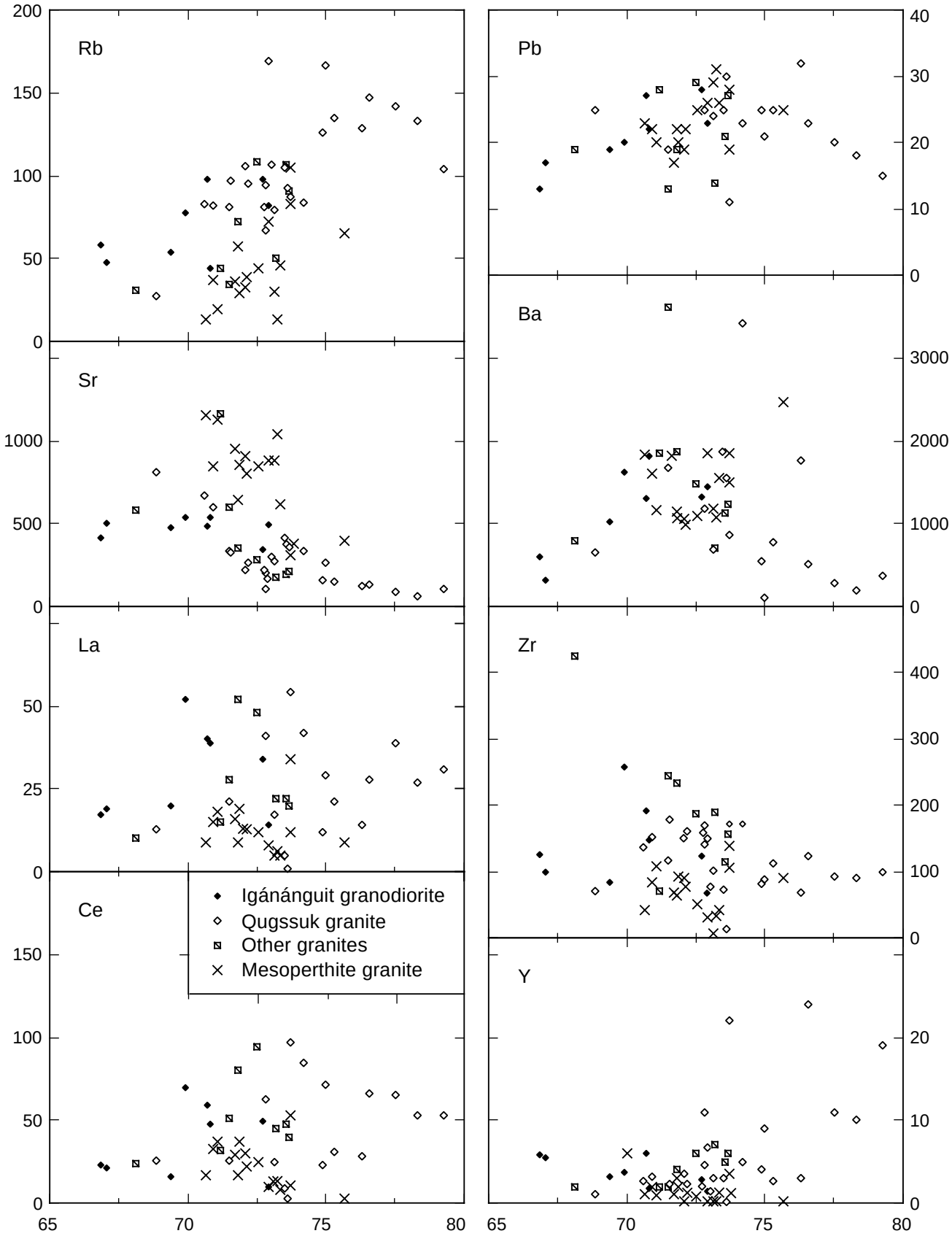

Fig. 74. Selected trace element variation diagrams against SiO_2 (in ppm and wt. %), granitic rocks, Fiskefjord area. See Appendix for analytical details. Sample localities shown in Fig. 68.

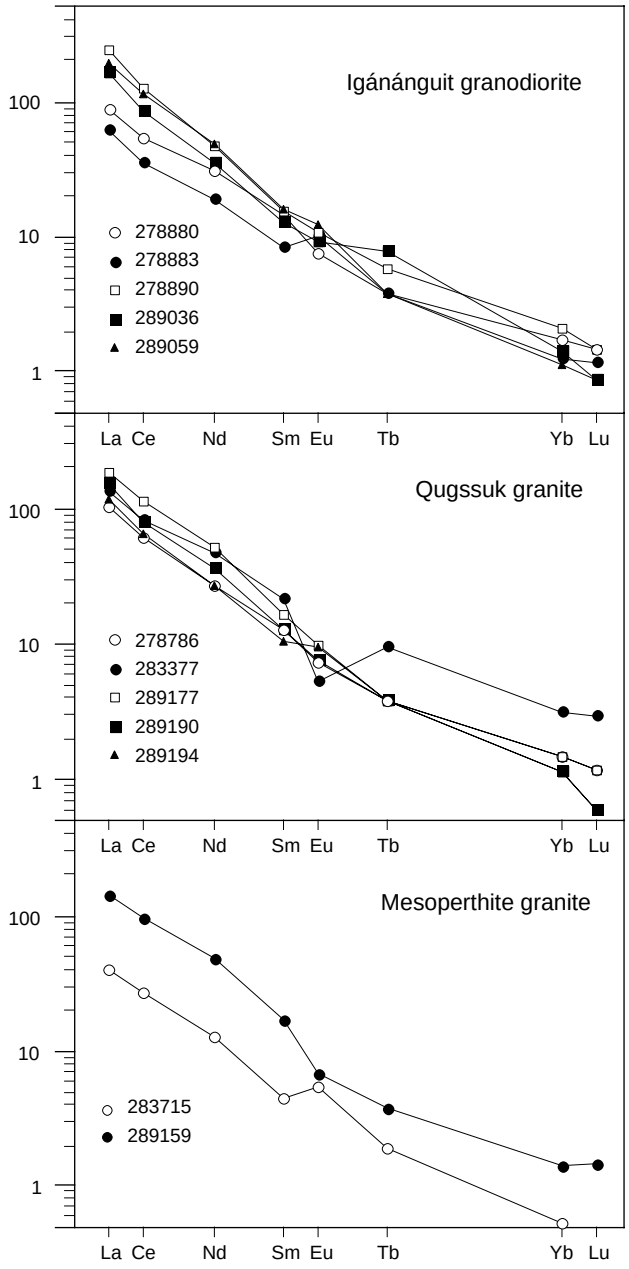

Fig. 75. Chondrite-normalised REE diagrams (Nakamura, 1974) of granitic rocks, Fiskefjord area. All elements analysed by INNA (see Appendix). Sample localities shown in Fig. 68.

Granodiorite and granite

Four different groups of granitoid rocks have been studied (sample locations shown on Fig. 68), namely the late-kinematic (a) Igánánguit granodiorite and (b) Qugssuk granite bodies, (c) a group of contemporaneous amphibolite facies granite sheets emplaced into granulite facies dioritic gneiss in north-eastern Nordlandet (referred to as 'other granites' on Fig. 68 and subsequent figures), and (d) synkinematic mesoperthite (granulite facies) granite sheets in the central and western parts of the Fiskefjord area. Representative and average chemical compositions of the four groups of granitoid rocks are presented in Appendixes 10–11.

Variation diagrams of major and trace elements against SiO_2 (Figs 73, 74) show that groups a–c outline more or less continuous compositional fields. Collectively they are comparable to the most K_2O-rich end members of Taserssuaq tonalite, but clearly different from the most acid members of the TTG suite of grey gneiss (lower MgO, FeO* and CaO, similar or lower TiO_2 and P_2O_5 contents, higher LIL trace element contents and higher K_2O/Na_2O ratios). Their chondrite-normalised REE patterns (Fig. 75) are highly fractionated and LREE-enriched – even more so than in tonalitic-trondhjemitic gneiss, with La >100 × chondrite and normalised La/Yb ratios of *c.* 100. Sample 283377 of Qugssuk granite has a different REE pattern and a large negative Eu anomaly, resembling the altered sample 289208 of Taserssuaq tonalite.

As previously noted the mesoperthite granite has a very felsic modal composition, almost entirely consisting of quartz and variably exsolved ternary feldspar. It has remarkably homogeneous major and trace element compositions which only partially overlap with those of the other granitoids (Figs 73, 74), and its relatively small internal variations are interpreted as solely reflecting variable modal proportions of quartz and feldspar. Most elements show distinct correlations with silica, which has a narrow range between *c.* 71 and 76 wt. % SiO_2 (Figs 73, 74). The rocks are very low in MgO and FeO* and high in Al_2O_3, and display a granitic trend despite relatively low K_2O/Na_2O ratios. Sr contents are very high, up to *c.* 1200 ppm, whereas Pb and Ba contents (*c.* 20–30 and 1000–2000 ppm, respectively) are comparable to those in groups a–c. Rb is low, rarely exceeding 50 ppm, and also the Zr, Y and REE contents (Figs 74, 75) are lower than in groups a–c. As in the other granitoid rocks the two available REE spectra from the mesoperthite granite are strongly fractionated (Fig. 75); they display both positive and negative Eu anomalies.

In terms of their major and trace element compositions all four groups of granite are comparable to Archaean I-type calc-alkaline orogenic granites, generally assumed to represent partial melts of crustal igneous precursors (e.g. Sylvester, 1994).

Discussion

Origin of tonalitic, trondhjemitic and granodioritic magmas

Field observations, petrography and geochemistry suggest that the amphibolite facies tonalitic-trondhjemitic grey gneisses and the late-tectonic, mainly amphibolite facies Finnefjeld and Taserssuaq complexes are the least altered members of grey gneiss *s.l.* in the Fiskefjord area. In the preceding sections it was shown that the compositions of these units strongly resemble average Archaean TTG *sensu* Condie (1981) or Martin (1994), specifically with respect to their low K_2O/Na_2O ratios, low FeO* + MgO + TiO_2 and comparatively high Al_2O_3 contents, relative depletions in mantle-normalised Nb, Ta and Ti compared to other elements, and highly fractionated REE spectra. In addition the low initial $^{87}Sr/^{86}Sr$ ratio of grey gneisses (*c.* 0.7020, Table 1) implies a short crustal residence before emplacement of their igneous precursors. These geochemical features, taken together, are now assumed by most authors to indicate an origin by partial melting of an amphibolite source with residual hornblende ± garnet. Several experiments (e.g. Winther & Newton, 1991; Rapp *et al.*, 1991) have shown that partial melting of a tholeiitic source at moderate pressures can produce large amounts of TTG melts – provided that the source is hydrated; besides, hornblende ± garnet ± titanite are capable of retaining HREE, Y, Nb, Ta and Ti in appropriate proportions to account for their observed concentrations in the TTG rocks (Saunders *et al.*, 1980; Green & Pearson, 1987).

The wide range of major element compositions in the TTG rocks indicate that the source magmas underwent significant modification by crystal fractionation before final emplacement. Dioritic and gabbroic plagioclase-hornblende enclaves in both the Finnefjeld gneiss and Taserssuaq tonalite complexes support this; it was shown above that (at least) the latter are likely to be cogenetic with the complex in which they are found. Besides, the two distinct sample populations from the Taserssuaq tonalite and Finnefjeld gneiss complexes show different major element variation trends against SiO_2, which are compatible with different degrees of plagioclase and hornblende fractionation in the two complexes.

Origin of common dioritic gneiss

The large proportion of mafic tonalite, quartz diorite and diorite in the grey gneiss of the Fiskefjord area is unusual compared with other parts of the Archaean block of West Greenland and with most other Archaean cratons, where dioritic or andesitic components are uncommon. Part of the dioritic gneiss is significantly older than the main TTG suite (Table 1). The less fractionated REE patterns and moderate Nb, Ta and Ti anomalies of the common dioritic gneiss compared to the tonalitic-trondhjemitic gneiss might indicate that the diorite melts were formed by unusually large degrees of partial melting of the supposed amphibolitic TTG source during an embryonic stage of continent formation. However, experiments have shown that bulk melting of amphibolite is not approached under realistic lower crust or upper mantle temperature and pressure conditions (e.g. Rapp *et al.*, 1991; Winther & Newton, 1991). It is therefore more likely that the magmatic precursor to the common dioritic gneiss was generated in a more complicated process, and that a significant component of mantle was involved; the compositional overlap between the diorite and the most leucocratic amphibolites of the supracrustal association might actually suggest this. Experiments e.g. by Green (1976) have shown that quartz-saturated diorites can be produced by *c.* 25% hydrous melting of peridotite, and as noted by Stern *et al.* (1989) natural diorite melts would probably be somewhat less mafic than the experimental melts, due to dissolved silica and LIL elements in the natural hydrous fluids. Assuming that plate tectonic processes were active in the Archaean (see p. 89), magmatic accretion of diorite could have taken place in a convergent plate-tectonic scenario similar to that suggested for modern island arc environments, with participation of a mantle wedge which was fluxed by hydrous fluids originating from the subducted slab. Also this model would require a residue containing hornblende ± garnet ± titanite in order to account for the observed Y, HREE and HFS element depletion in the dioritic gneiss.

Origin of the Qeqertaussaq diorite

As already shown the Qeqertaussaq diorite and immediately adjacent tonalitic gneiss have low TiO_2, MgO, FeO*, CaO, Nb, Cr, Ni and V contents, high to very high Na_2O, K_2O, P_2O_5, Pb, Ba, Sr and LREE contents, and relatively high K/Rb ratios compared with the common grey gneiss or average TTG suites. Some of these characteristics, notably enrichment of Sr and Ba, are also known from other, more leucocratic basement rocks elsewhere in West Greenland, namely from certain

Archaean granitoids in the Disko Bugt region (A. Steenfelt, personal communication, 1995) and from Proterozoic orthogneiss units in the central part of the Nagssugtoqidian orogen (F. Kalsbeek, personal communication, 1995). In terms of LIL element compositions, but not with regard to compatible elements such as Mg, Cr and Ni, the Qeqertaussaq diorite also resembles some modern high-Mg andesites (sanukitoids, Tatsumi & Ishizaka, 1982; bajaites, Saunders *et al.*, 1987), certain Caledonian lavas and granitoids of West Scotland (Stephens & Halliday, 1984; Tarney & Jones, 1994), and Archaean sanukitoids and associated granitoids described by Stern *et al.* (1989) from the Superior Province in Canada. There are also clear similarities with LIL element and P_2O_5-enriched, HFS element-depleted (e.g. Nb, Ti) dioritic members of the Late Archaean Skjoldungen alkaline igneous province in southern East Greenland (Blichert-Toft *et al.*, 1995). Contrary to the Qeqertaussaq diorite, most of the latter suites of rocks are late tectonic, interpreted by the respective authors as having had a large component of primitive or fluid-enriched mantle in their sources, and hornblende fractionation is commonly supposed to have taken place at some stage in their formation. Blichert-Toft *et al.* (1995) argued that the Skjoldungen province has a chondritic mantle signature rather than having been derived from recycled older sediments.

Due to the low Mg/Fe ratios and low concentrations of MgO, Cr, Ni and related trace elements in the Qeqertaussaq diorite, an interpretation which implies a large component of enriched mantle in the end product, is not viable. Amphibolite melting is ruled out because it is not supported by experimental data and furthermore could not produce sufficiently high concentrations of, e.g. Sr and Ba, in the diorite. A purely metamorphic origin of the anomalous composition of the Qeqertaussaq diorite is also not favoured.

The Qeqertaussaq diorite probably had a multistage origin, in which localised mantle metasomatism may have played an important role prior to the formation of a diorite melt. Assuming that the source of the Qeqertaussaq diorite comprised a large mantle component, it would have to be strongly enriched in P_2O_5, Sr, Ba, other LIL elements and LREE. It is considered unlikely that this enrichment could have been achieved during partial melting of the upper mantle, solely by hydrous fluids released into the mantle from recycled crustal sediments or amphibolites; a process of this type might also be expected to have a more regional influence than observed. However, more intense and more localised mantle metasomatism may take place if the mantle comes into contact with carbonatite melts. Experiments with dolomitic melts at upper mantle temperatures and pressures (Green & Wallace, 1988) and studies of carbonated mantle peridotite xenoliths in volcanic rocks (e.g. Ionov *et al.*, 1993) have shown that ephemeral carbonatite melts in the upper mantle can produce very effective LIL element and LREE enrichment and HFS element depletion in spinel peridotite, whereby enstatite is transformed to magnesian diopside or pargasite but Mg/Fe ratios remain largely unchanged. Dolomitic carbonatite melts can coexist with pargasite-bearing lherzolite at *c.* 25 kbar, 1000°C, whereby extensive trace element exchange can take place between carbonate and silicate phases, and new LREE-enriched apatite can be formed. The HFS elements Ti, Nb and Ta are retained in the amphibole. Subsequent decarbonation (without carbonatite magma eruption) may occur from the metasomatised mantle under pressures less than 21 kbar at 950–1050°C, and could conceivably have taken place prior to partial hydrous melting of the enriched mantle.

In support of the proposed localised mantle metasomatism prior to diorite formation it can be noted that two carbonatites (one Late Archaean, one Late Proterozoic) and a number of Late Proterozoic kimberlite dykes are known from the northern part of the Archaean block in southern West Greenland adjacent to the Fiskefjord area (Larsen & Rex, 1992). However, it has not been established if this 'carbonatite-kimberlite province' can be extended back to the earliest history of the region.

Origin of the granitic rocks

It has been shown that the Igánánguit granodiorite, Qugssuk granite and also the mesoperthite granite sheets geochemically belong to the I-type of calc-alkaline granites which are generally assumed to represent late orogenic partial melts of crustal igneous precursors.

In his recent compilation of Archaean granites, Sylvester (1994) subdivided Archaean calc-alkaline granites from eight cratons worldwide into two subgroups, CA_1 and CA_2, the former with higher mean Y, TiO_2, FeO, MgO, CaO, P_2O_5, Sc, V, Zr, REE and Ta, and lower mean Na_2O and Cr concentrations. He argued that the quoted compositional differences are mainly due to different crustal depths of the source areas (viz. pressures of *c.* 6 and 10 kbar), where garnet and hornblende would only occur as restite phases to the group CA_2. He also argued that the CA_2 group, potentially

having had a greater distance available to rise in the crust, would generally be more effectively separated from restite minerals (and hence have the more felsic composition of the two groups).

Except for Cr contents which are always very low (1–20 ppm) all granite groups in the Fiskefjord area would chemically belong to group CA_2 of Sylvester (1994), with the mesoperthite granite providing the best fit. It seems reasonable from granite field relationships and *P-T* estimates of the granulite facies metamorphism in the southern part of the Akia terrane (Reed, 1980; Pillar, 1985; Riciputi *et al.*, 1990) that the granites could have been melted from sources at pressures up to *c.* 10 kbar. In addition, the fact that the granites have more fractionated REE patterns than the grey gneiss supports the idea that hornblende ± garnet were important restite phases, assuming that the granitic melts were indeed separated from a source of grey gneiss.

Granulite facies metamorphism, retrogression and element mobility in grey gneiss

Granulite facies metamorphism

Granulite facies metamorphism extends over the south-western part of the Akia terrane, including Nordlandet and a large part of the Fiskefjord area, whereas the easternmost part of the Fiskefjord area (and of the Akia terrane) consists of upper amphibolite facies rocks that have not experienced granulite facies metamorphism. Large tracts between these two areas are variably retrogressed (Fig. 76). Whole-rock Pb-Pb ages of 3000 ± 70 Ma (Taylor *et al.*, 1980) and 3112 ± 40 Ma (Garde, 1989a) obtained from orthogneiss in Nordlandet and the eastern part of the Fiskefjord area have been interpreted to date the granulite facies metamorphism; a 2999 ± 4 Ma SHRIMP age of metamorphic zircon overgrowth in a garnet-sillimanite-bearing metasediment from Nordlandet just south of the Fiskefjord area (Friend & Nutman, 1994) firmly establishes that the peak of granulite facies metamorphism occurred at *c.* 3000 Ma, i.e., it culminated during or just after emplacement of the main phase of grey tonalitic-trondhjemitic gneiss. SHRIMP zircon data from Nordlandet dioritic gneiss reported in Table 1 and Fig. 25 suggest that this unit also experienced an earlier thermal event at *c.* 3180 Ma. The *c.* 3000 Ma granulite facies metamorphism outlasted two phases of isoclinal folding and a phase of upright, more open folding (the Pâkitsoq phase, Berthelsen, 1960) in the western and central parts of the Fiskefjord area. Granulite facies metamorphism appears to have overlapped with doming, and was succeeded by localised ductile deformation and emplacement of small granodiorite and granite plutons and granite sheets in the northern and eastern parts of the area.

Physical conditions of metamorphism

In Nordlandet the peak of metamorphism occurred under *P-T* conditions of *c.* 850°C, 8 kbar (Reed, 1980; Riciputi *et al.*, 1990), and at Langø, a small island west of Tovqussap nunâ, *c.* 825°C and 8.3 kbar were reported by Dymek (1984). Titanium-rich hornblende and biotite appear to have been stable throughout the granulite facies event in suitable rock types (Garde, 1990 and this paper), indicating that complete dehydration did not take place. According to Pillar (1985) and Riciputi *et al.* (1990) granulite facies metamorphism took place without free fluids, and fluid inclusion data from grey gneiss in the Fiskefjord area seem to support this (Garde, 1990). However, some aspects of the granulite facies rocks may be ascribed to fluid activity during the granulite facies event, for instance hornblende-bearing mafic pegmatites on Nordlandet in which 'high-grade' hornblende partially replaces orthopyroxene (McGregor *et al.*, 1986; McGregor, 1993); also the geochemistry of granulite facies biotite (p. 63) may suggest the former presence of metamorphic fluids (see p. 78).